

Challenging terrestrial biosphere models with data from the long-term multifactor Prairie Heating and CO₂ Enrichment experiment

MARTIN G. DE KAUWE¹ , BELINDA E. MEDLYN² , ANTHONY P. WALKER³, SÖNKE ZAEHLE⁴, SHINICHI ASAO⁵, BERTRAND GUENET⁶, ANNA B. HARPER⁷, THOMAS HICKLER^{8,9}, ATUL K. JAIN¹⁰, YIQI LUO¹¹, XINGJIE LU¹², KRISTINA LUUS⁴, WILLIAM J. PARTON⁵, SHIJIE SHU¹⁰, YING-PING WANG¹², CHRISTIAN WERNER⁸, JIANYANG XIA¹³, ELISE PENDALL², JACK A. MORGAN¹⁴, EDMUND M. RYAN¹⁵ , YOLIMA CARRILLO², FEIKE A. DIJKSTRA¹⁶, TAMARA J. ZELIKOVA¹⁷ and RICHARD J. NORBY³

¹Department of Biological Science, Macquarie University, North Ryde, NSW 2109, Australia, ²Hawkesbury Institute for the Environment, Western Sydney University, Locked Bag 1797, Penrith, NSW 2751, Australia, ³Environmental Sciences Division and Climate Change Science Institute, Oak Ridge National Laboratory, P.O. Box 2008, Oak Ridge, TN 37831, USA,

⁴Biogeochemical Integration Department, Max Planck Institute for Biogeochemistry, Hans-Knöll-Str. 10, 07745 Jena, Germany,

⁵Natural Resource Ecology Laboratory, Colorado State University, Fort Collins, CO 80523-1499, USA, ⁶Laboratoire des Sciences du Climat et de l'Environnement, LSCE/IPSL, CEA-CNRS-UVSQ, Université Paris-Saclay, F-91191 Gif-sur-Yvette, France,

⁷College of Engineering, Mathematics, and Physical Sciences, University of Exeter, Exeter EX4 4QF, UK, ⁸Senckenberg Biodiversity and Climate Research Centre (BiK-F), Senckenberganlage 25, 60325 Frankfurt, Germany, ⁹Department of Physical Geography, Geosciences, Goethe-University, Altenhöferallee 1, 60438 Frankfurt, Germany, ¹⁰Department of Atmospheric Sciences, University of Illinois, 105 South Gregory Street, Urbana, IL 61801-3070, USA, ¹¹Department of Microbiology and Plant Biology, University of Oklahoma, Norman, OK 73019, USA, ¹²CSIRO Oceans and Atmosphere, Private Bag #1, Aspendale, Vic. 3195, Australia, ¹³Tiantong National Forest Ecosystem Observation and Research Station, School of Ecological and Environmental Sciences, East China Normal University, Shanghai 200062, China, ¹⁴Rangeland Resources Research Unit, Agricultural Research Service, United States Department of Agriculture, Fort Collins, CO 80526, USA, ¹⁵Lancaster Environment Centre, Lancaster University, Lancaster LA1 4YW, UK, ¹⁶Centre for Carbon, Water and Food, School of Life and Environmental Sciences, The University of Sydney, Sydney, NSW 2006, Australia, ¹⁷Department of Botany, University of Wyoming, Laramie, WY 82071, USA

Abstract

Multifactor experiments are often advocated as important for advancing terrestrial biosphere models (TBMs), yet to date, such models have only been tested against single-factor experiments. We applied 10 TBMs to the multifactor Prairie Heating and CO₂ Enrichment (PHACE) experiment in Wyoming, USA. Our goals were to investigate how multifactor experiments can be used to constrain models and to identify a road map for model improvement. We found models performed poorly in ambient conditions; there was a wide spread in simulated above-ground net primary productivity (range: 31–390 g C m⁻² yr⁻¹). Comparison with data highlighted model failures particularly with respect to carbon allocation, phenology, and the impact of water stress on phenology. Performance against the observations from single-factors treatments was also relatively poor. In addition, similar responses were predicted for different reasons across models: there were large differences among models in sensitivity to water stress and, among the N cycle models, N availability during the experiment. Models were also unable to capture observed treatment effects on phenology: they overestimated the effect of warming on leaf onset and did not allow CO₂-induced water savings to extend the growing season length. Observed interactive (CO₂ × warming) treatment effects were subtle and contingent on water stress, phenology, and species composition. As the models did not correctly represent these processes under ambient and single-factor conditions, little extra information was gained by comparing model predictions against interactive responses. We outline a series of key areas in which this and future experiments could be used to improve model predictions of grassland responses to global change.

Keywords: allocation, carbon dioxide, FACE, grassland, models, PHACE, phenology, soil moisture, temperature

Received 14 November 2016 and accepted 15 January 2017

Correspondence: Martin G. De Kauwe, Department of Biological Sciences, Macquarie University, North Rydes, NSW 2109, Australia, tel. +61 2 9850 9256, fax +61 2 9850 8245, e-mail: mdekauwe@gmail.com

Introduction

Grasslands are estimated to cover 20% of the terrestrial land surface (Lieth, 1978; Hadley, 1993) and store ~25% of the world's soil carbon (C) excluding permafrost

soils (Jobbágy & Jackson, 2000; Ciais *et al.*, 2013). However, whether grasslands will be substantial C sources or sinks in the future is uncertain; estimates of future C uptake range between -2 and 2 Gt C yr⁻¹ (Scurlock & Hall, 1998). Semi-arid ecosystems, including grasslands, are large contributors to both the trend and interannual variability in above-ground net primary production (Knapp & Smith, 2001) and net biome production (Ahlström *et al.*, 2015), over the last three decades, suggesting these ecosystems are particularly important for accurately predicting terrestrial C-cycle responses to global change.

To predict how increasing temperatures, atmospheric carbon dioxide (CO₂) and changing precipitation patterns will affect ecosystem function and species composition, multifactor ecosystem-scale experiments have been widely advocated (Heimann & Reichstein, 2008; Luo *et al.*, 2008; Leuzinger *et al.*, 2011). As global change factors likely cause a series of complex interactions (Fuhrer, 2003; Hovenden *et al.*, 2014), single-factor experiments may not be sufficient to investigate future ecosystem-scale responses. Further, while interactive effects are typically smaller than main effects (Shaw *et al.*, 2002; Dieleman *et al.*, 2012), they may sometimes exceed single-factor effects. However, interactive effects may be contingent on environmental conditions, such as interannual variability in precipitation (Mueller *et al.*, 2016). As a result, multifactor experiments can be more difficult to interpret, and underlying mechanisms harder to identify, than single-factor experiments.

For example, Shaw *et al.* (2002) found contrasting results when comparing responses from single and multifactor treatments in the Californian grasslands at the Jasper Ridge Global Change Experiment (JRGCE). In the third year of the experiment, net primary productivity (NPP) was increased in response to elevated CO₂ (eCO₂). However, the interactive effect of multifactors suppressed the NPP response seen in the single-factor response. Re-examining the responses at the JRGCE over 5 years, Dukes *et al.* (2005) concluded that NPP did not in fact respond to eCO₂. Hovenden *et al.* (2008) also found no CO₂ enhancement in ecosystem productivity in an Australian perennial grassland experiment (TasFACE). This lack of response was attributed to a reduction in soil N availability in response to eCO₂, but increasing temperature by 2 °C in combination with the CO₂ treatment was found to prevent this decrease in available N. In the multifactor Prairie Heating and CO₂ Enrichment (PHACE) experiment, Mueller *et al.* (2016) found that above-ground NPP and total plant biomass both had time-dependent and interactive effects of warming and eCO₂. Above-ground NPP responses to the combination of eCO₂ and warming exceeded responses to the single factors

(nonadditive). Soil moisture was especially important in explaining the productivity responses to treatments as well as interannual precipitation variability.

Dieleman *et al.* (2012) conducted a meta-analysis using data from 150 manipulation experiments and concluded that the response of above-ground biomass to the combined treatments of CO₂ and warming was typically less than additive. These results suggest that single-factor experiments, which miss the interaction, may overestimate responses, highlighting the need to test models against multifactor experiments. However, model comparisons to date have only explored theoretical multifactor experiments (e.g. Melillo *et al.*, 1993; Riedo *et al.*, 1997; Pepper *et al.*, 2005; Parton *et al.*, 2007; Luo *et al.*, 2008), rather than applying models directly to experimental data.

The model-data intercomparison approach has been useful to investigate single-factor forest experiments (De Kauwe *et al.*, 2013, 2014; Zaehle *et al.*, 2014; Medlyn *et al.*, 2015; Walker *et al.*, 2015), but it is not clear whether multifactor experiments will be as useful to constrain models when their responses seem so diverse and, in dry environments, contingent on environmental conditions. In this study, we applied 10 state-of-the-art terrestrial biosphere models (TBMs) to an 8-year, multifactor (CO₂ × warming) grassland experiment. Our goals were to (i) explore how a multifactor experiment can be used to constrain models and (ii) identify ways to improve models based on this experiment.

Materials and methods

Site description

The PHACE experiment was located in the semi-arid grasslands of Wyoming, USA (41.18°N, 104.9°W), was established in 2006, and lasted 8 years. Mean winter and summer temperature at the site were -2.5 °C and 17.5 °C, respectively, with a mean annual precipitation of 403 mm (range: 224–496 mm). The site has marked variation in both annual and growing season precipitation (Fig. 1). The site was previously subject to grazing, but was fenced off in 2005. Vegetation at the site is dominated by C₃ grasses (55%), with C₄ grasses constituting 25% and the final 20% made up of sedges, forbs, and small shrubs.

The experiment implemented a factorial combination of warming (+1.5 °C during the day; +3.0 °C at night) and elevated CO₂ (600 ppm; ambient = 385 ppm), with five replicates per treatment. The elevated CO₂ treatment, initiated in 2006, used Free Air CO₂ Enrichment (FACE) technology (Miglietta *et al.*, 2001). The warming treatment, initiated a year later in 2007, used infrared heaters (Kimball, 2005). In the first year (2006), an additional 160 mm of water was added (20 mm × 8 dates during the growing season) to establish growth. Further details can be found in Morgan *et al.* (2011), Pendall *et al.* (2013), Ryan *et al.* (2015), and Zelikova *et al.* (2015).

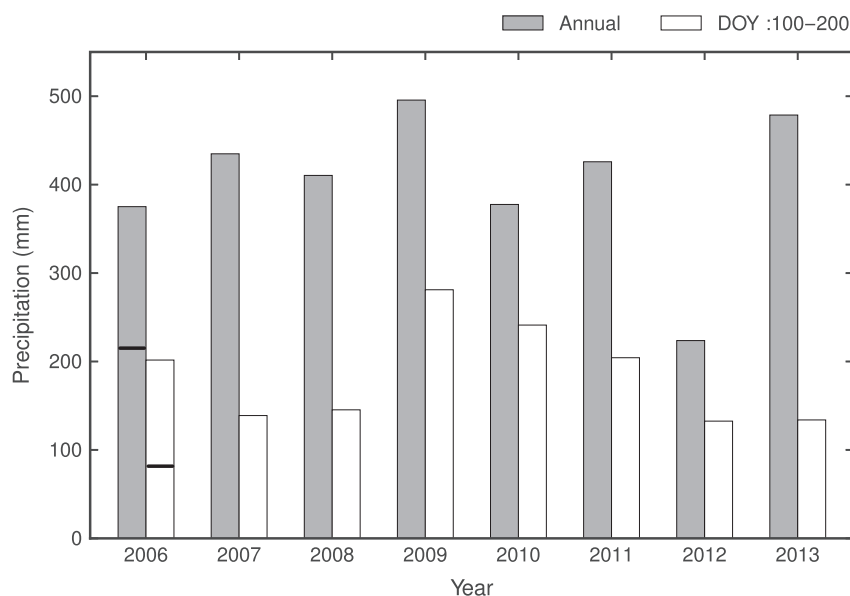


Fig. 1 Annual and early- to mid-growing season (day of year: 100–200) when soil water availability most limits productivity (Morgan *et al.*, 2011). In 2006, all plots were irrigated (20 mm × 8) with 160 mm of additional water. The additional water is shown by the precipitation above the black horizontal line in 2006. The annual bar shows the effect of the eight additional treatments, whereas the early- to mid-growing season bar shows the addition of the six treatments which occurred during that period.

Summary of the experimental findings

Mueller *et al.* (2016) present a comprehensive summary of the ecosystem responses over the duration of the PHACE experiment. Elevated CO₂ effects on soil water content usually counteracted the desiccating effect of warmer temperatures. However, the combination of eCO₂ and elevated temperature tended to enhance soil water content early in the experiment, but reduced it after 7 years of treatment when compared to control plots under present-day CO₂ and temperature levels. Above-ground plant biomass responded positively to eCO₂ and eCO₂ combined with warming, especially in dry years when water savings were most important to growth. In contrast, while above-ground biomass did not respond to warming alone, root biomass responded positively to both warming and eCO₂, but only in wetter years, with either eCO₂ or warming enhancing production approximately 30% in wet growing seasons. As a result, total plant biomass responded consistently and positively to eCO₂ alone or combined with warming, with a 25% increase observed in the combined treatment compared to control plots. The positive effect of the combined eCO₂ and warming on above-ground plant biomass with passing years was increasingly experienced by C₃ grasses, reversing biomass responses in the first few years of the experiment when C₄ grasses were favoured (Morgan *et al.*, 2011). Soil nitrate availability was enhanced by warming and reduced by eCO₂, although contrasting effects were observed for soil ammonium (Carrillo *et al.*, 2012). In contrast, wetter soil conditions under eCO₂ increased phosphorus (P) availability to plants and microbes relative to that of N, while drier conditions with warming reduced P availability relative to N (Dijkstra *et al.*, 2012). Warming combined with eCO₂ extended the

seasonality of plant activity (greenness), especially because of earlier spring growth with warming (Zelikova *et al.*, 2015).

Experimental data

To constrain the models, we used five key data sets: (i) above- and below-ground biomass; (ii) shoot and root N concentrations; (iii) vegetation greenness; (iv) leaf-on/off dates; (v) soil water content.

Plant biomass (above- and below-ground) and N concentrations (elemental analyser) were measured in mid-July as biomass reached its maximum (Morgan *et al.*, 2011; Dijkstra *et al.*, 2012; Carrillo *et al.*, 2014). Above-ground biomass measurements were obtained by clipping vegetation that resided in the harvest areas (1.5 m² harvest area, but clipping 50% of this area each year from alternating grids). Root-biomass measurements were obtained from cores taken to a depth of 15 cm. These data exclude below-ground crown tissues estimates (see Discussion). Above-ground biomass estimates were corrected using pretreatment data from 2005 to account for initial differences between treatment plots and control plots (see Morgan *et al.*, 2011; also Mueller *et al.*, 2016).

Vegetation greenness was inferred from biweekly digital photographs taken between March and October. In 2008, photographs were obtained monthly (see Zelikova *et al.* (2015) for details). Phenology leaf-on and leaf-off dates for different species were obtained by direct observation (Reyes-Fox *et al.*, 2014).

Soil moisture measurements were taken hourly using EnviroSMART probes at 10 and 20 cm soil depths. These data were

combined to give a total estimate of soil water content in the top 25 cm.

Models

The 10 process-based models applied to the PHACE experiment contrasted markedly in terms of application, complexity, and structure. Broadly, they can be considered to encompass three categories: stand (DAYCENT, GDAY), land surface (CABLE, CLM4.5, ISAM, O-CN, ORCHIDEE), and dynamic vegetation models (JULES, LPJ-GUESS, SDGVM). A detailed overview of eight of these models and how they differ in terms of key assumptions can be found in Walker *et al.* (2014), with detailed analyses of their water and N cycle responses to eCO₂ found in De Kauwe *et al.* (2013) and Zaehle *et al.* (2014), respectively. The two models not described in these previous analyses, JULES and ORCHIDEE, are fully documented in Clark *et al.* (2011) and Krinner *et al.* (2005), respectively. Here, we provide some basic assumptions in relation to growth and phenology used in each of the models that affects simulations of the PHACE experiment (see Table 1).

Modelling simulations

Model participants submitted simulations covering the experimental period (2006 – 2013) for the ambient (ct), eCO₂ (Ct), warming (cT), and eCO₂ × warming (CT) experiments. Models were spun-up to equilibrium (2000 year minimum) using their standard spin-up approach accounting for site history and using a fixed CO₂ concentration of 285 μmol mol⁻¹ and fixed N deposition set at the 1850 value based on Dentener *et al.* (2006). Models estimated biological N fixation (BNF) following their standard approach: CABLE uses a method based on light, N, and phosphorus availability (Wang *et al.*, 2009; BNF was estimated to be zero for the site), CLM4.5 uses an empirical relationship based on NPP (Oleson *et al.*, 2013), DAYCENT estimates N fixation as a function of climate (Parton *et al.*, 1987), and GDAY, ISAM, LPJ-GUESS, and O-CN use an empirical relationship with long-term evapotranspiration (Cleveland *et al.*, 1999). Modellers were provided with stand and soil characteristics to parameterize their models so as to be representative without being 'tuned' to the observations. Examples of these data include tissue C:N ratios, the maximum carboxylation rate, specific leaf area, and tissue lifespans. In addition, models were provided with information on the rooting depth, the field capacity, and wilting point to ensure that they represented the same effective soil water buckets.

Experimental plots were harvested (mid-July) to simulate grazing; by contrast, models did not assume any site disturbance during simulations. This choice was made because harvested plant biomass was removed from a small area of the plot only, while some of the experimental data did not come from the harvest areas (e.g. root biomass, soil moisture). Models, including dynamic vegetation models (JULES, LPJ-GUESS, and SDGVM), did not simulate competition among plant functional types. Instead, models simulated the sites by weighting outputs by the average observed ambient total C₃ and C₄ above-ground biomass fractions, 0.69 and 0.31, respectively.

Data availability is summarized at <https://facedata.ornl.gov/facemds/>.

Results

Ambient CO₂

While the models are able to capture the observed interannual variability in above-ground net primary productivity (aNPP; Fig. 2), $r > 0.86$, there is a wide spread in the magnitude of simulated values (RMSE mean across models = 96 g C m⁻² yr⁻¹; range: 31–390 g C m⁻² yr⁻¹). To explain differences among the models, we analysed aNPP by decomposing the modelled aNPP flux into its average component parts (see Equation 1 and Table 2). Each of these component terms is a simplification of how the models operate, but on an annual time step should closely approximate simulated aNPP fluxes, allowing us to better understand causes of differences among models. aNPP can therefore be analysed as:

$$\text{aNPP} = A_b \cdot \text{CUE} \cdot \text{GPP}_u \cdot \beta \cdot \text{LAI}_p \cdot \text{LAI}_r,$$

where A_b is the allocation of net primary productivity above-ground (fraction), CUE is the C-use efficiency, or the fraction of gross primary productivity (GPP) not lost as respiration (fraction); GPP_u is the unstressed GPP per unit leaf area (g C m⁻² leaf⁻¹ day⁻¹); β is the water stress factor which limits productivity as water content declines (fraction); LAI_p is the peak LAI value in a year (m⁻² leaf m⁻² ground); and LAI_r is the integral of LAI over the year divided by the peak LAI (LAI_p) and indicates LAI duration (day yr⁻¹). GPP_u is inferred from model output by dividing GPP by ($\beta \cdot \text{LAI}_p \cdot \text{LAI}_r$).

The size of the spread in component terms across models is greater than the aNPP spread between models, which suggests that models are arriving at the same answer for different reasons (Table 2). For example, DAYCENT and GDAY predict similar average aNPP values, but to get to this prediction, GDAY has a low GPP_u (4.71 g C m⁻² leaf⁻¹ day⁻¹) and a high β (low water stress; 0.73). By contrast, DAYCENT has a much greater GPP_u (11.92 g C m⁻² leaf⁻¹ day⁻¹) but a very low β (0.17). The most variable components among models are as follows: (i) LAI_r (range: 77–256 days); (ii) LAI_p (range: 1.21–6.1 m² m⁻²); (iii) A_b (range: 0.16–0.92); and (iv) β (range: 0.17–0.97). We now examine each of these components in more detail.

Leaf area index (LAI_r and LAI_p)

Observed seasonal phenology at the site, inferred from greenness estimates, corresponds with measured soil water content (SWC; 5–15 cm; Fig. 3). Drops in

Table 1 Summary of model phenology and growth assumptions. C is carbon, GDD is the number of growing degree-days, GDD5 is the number of growing degree-days above 5 °C, GPP is gross primary productivity, LAI is leaf area index, maxGDD is the a maximum growing degrees-day threshold, N is nitrogen, NPP is net primary productivity, PAR is the photosynthetically active radiation, SLA is the specific leaf area, and SWI is soil water index

Models	Leaf onset	Growth	Leaf drop	References
CABLE	Leaf onset is prescribed based on a satellite climatology, implying no interannual variability. Onset dates vary as a function of latitude	After leaf onset, 80% of NPP is allocated to leaves for a 2-week period. Following this 2-week period, allocation to leaves is reduced to 20% of NPP until 2 weeks prior to leaf drop, at which point NPP allocation to leaves is 0	Leaf drop is prescribed based on a satellite climatology, implying no interannual variability. Drop dates vary as a function of latitude	Zhang (2004)
CLM4.5	For grasses, leaf onset begins after (i) exceeding a GDD sum of days >0 °C in the third soil layer, the GDD threshold for onset is a function of the 2 m mean annual temperature (MAT at 2 m); (ii) a SWI accumulation threshold (15 MPa days; accumulated matrix potential above a 'onset' minimum: -2 MPa, in the third soil layer), and (iii) day length (>6 h). Onset can occur multiple times in a year if the conditions are met following an offset period	Taken from transfer pool at a linearly decreasing rate.	Leaf drop occurs due to (i) a sustained period of dry soil (-5 MPa days; accumulated matrix potential below an 'offset' maximum, -2 MPa, in the third soil layer); (ii) cold temperature (-15 GDD threshold of days below zero); or (iii) day length <6 h	Oleson <i>et al.</i> (2013)
DAYCENT	Leaf onset is prescribed to occur at a fixed date	After growth begins, carbon for leaf and root growth is taken from carbon stored in previous year growing season. Peak growth is determined by temperature, water, and nutrient availability, and prescribed maximum LAI that controls leaf death due to shading	Leaf drop is prescribed	Parton <i>et al.</i> (1993)
GDAY	Growth begins after exceeding both a precipitation and a GDD threshold. The precipitation threshold is 15% of the annual precipitation. GDD are	For deciduous species, leaf growth comes from carbon stored in the previous year growing season. It is assumed that all growth occurs before	Day of year ≥ 243 and mean daily air temperature is above 0 °C for cool and for 5 °C warm grasses Soil water availability has no effect on	Foley <i>et al.</i> (1996), White <i>et al.</i> (2000), Botta <i>et al.</i> (2000)

Table 1 (continued)

Models	Leaf onset	Growth	Leaf drop	References
	calculated from the sum of mean daily air temperature above 0 °C for cool-season grasses (temperature range > 20 °C or minimum temperature >= 5 °C) and 5°C warm-season grasses (temperature range <= 20 °C and minimum temperature <5 °C) grasses. The thresholds are 185 and 400 days for C ₃ and C ₄ grasses, respectively	the mid-point of the growing season, after this point senescence begins. Both growth and litterfall occur with a linearly ramping rate. These assumptions result in a symmetrical growth dynamic	litterfall in the deciduous model	
ISAM	Growth begins when (i) the daily mean root-zone temperature is >10 °C for 14 consecutive days, and (ii) the day length is >12 h	There are two growth stages: (i) the maximal growth stage, where more carbon is allocated to foliage to capture light and (ii) the normal growth stage, where more carbon is allocated to roots/stem to acquire resources. Plants enter then normal growth stage when their LAI exceeds half of their potential maximum LAI (set to 3) In addition, if grassland enters the leaf drop stage due to water stress, they may return to the growth stage if the water stress falls below 40% and other conditions for leaf onset are still satisfied	Leaf drop occurs when at least one of the following four conditions is met: (i) water stress is >40% for 14 consecutive days, (ii) the daily mean root-zone temperature is <10 °C and the day length <12 h, (iii) the LAI is > than the potential maximum LAI (set to 3), and (iv) plant maintains the normal growth phase for longer than 120 days	Song <i>et al.</i> , (2013), El Masri <i>et al.</i> , (2015)
JULES	Growth begins when the canopy temperature (T _c) is above a threshold (5 °C)	The rate of growth is $G_p(1-L_b)$, where G_p is a parameter (20 yr ⁻¹), and L_b is the 'balanced LAI', or the LAI the plant would have in full leaf (allometrically related to height). Growth continues as long as the plant is assimilating carbon, until leaf area index	When T _c drops below the threshold temperature, leaf turnover rate is modified (see eq. 47 in Clark <i>et al.</i>)	Clark <i>et al.</i> (2011) – See Section 4; Cox <i>et al.</i> (2001)

Table 1 (continued)

Models	Leaf onset	Growth	Leaf drop	References
LPJ-GUESS	For grasses, leaf onset begins after exceeding a GDD sum threshold (0)	reaches L_b , while $T_c > \text{threshold } T$ Growth is calculated at the end of a year. The annually integrated NPP is then allocated to leaves and roots, with a higher fraction allocated to roots under water and/or nitrogen limitation. Grasses are inactive under cold or very dry conditions. The maximum LAI (as calculated by carbon mass for leaves at the end of the previous year divided by a SLA) is scaled with a phenology development factor ($GDD5/\text{maxGDD}$; $\text{maxGDD}=100$). For grasses, this scalar is also zero at any days where plant-available soil water content falls below 35% of water-holding capacity	Once a 30-day running average temperature falls below a threshold (5°C), the cumulative GDD5 counter is reset. In the simulation, we also introduced a 60-day inhibition for the GDD5 counter preventing immediate increase after the senescence event was triggered	Smith <i>et al.</i> (2014)
O-CN	Growth begins after exceeding a GDD threshold above 5°C , subject to weekly moisture above 25% of field capacity and a positive trend in weekly soil moisture. The GDD requirement adjusts to long-term annual mean temperature and was applied here at a value of 270 and 400 days for C_3 and C_4 grasses, respectively	Growth is modelled using a functional balance approach between leaves, tillers, and fine roots, responding to moisture and N status. Growth is fuelled from a labile carbon pool, which is filled by current photosynthetic carbon uptake and a long-term reserve (past GPP). Once the incremental net carbon gain of the canopy goes negative, most growth is allocated to seed production	The turnover time of leaves increases once weekly temperatures drop below $-2/2^\circ\text{C}$ (for C_3/C_4 grasses respectively) and weekly soil moisture below 10% of field capacity. Complete abscission within 10 days commences once weekly NPP becomes negative	Krinner <i>et al.</i> (2005), Zaehle & Friend (2010), with unpublished updates
ORCHIDEE	The leaf onset scheme follows Botta <i>et al.</i> (2000). Leaf onset for tropical grasses begins 35 days after the dry season	Leaf growth draws from stored carbon reserves initially until GPP is sufficient to support leaf growth.	Two different criteria are used separately to calculate the fraction of dying leaves at each time step: (i) a	Friedlingstein <i>et al.</i> (1998); Botta <i>et al.</i> (2000)

Table 1 (continued)

Models	Leaf onset	Growth	Leaf drop	References
	moisture availability minimum. For boreal regions, the number of GDD during the dormancy season has to exceed a prescribed threshold (185). For temperate grasses, both criteria (i.e. elapsed number of day and GDD threshold) control the leaf onset	Carbon fixed through photosynthesis is redistributed following the allocation scheme developed by Friedlingstein <i>et al.</i> , (1998). This allocation scheme is controlled by biophysical limitations (light, water)	meteorological criterion controlled by temperature and water stress (temperature <4 °C for C ₃ and 5 °C for C ₄ grasses; moisture >20% for both), and ii) the leaf age itself (>120 days)	
SDGVM	For evergreen vegetation, leaf onset is triggered by a GDD accumulation, threshold (110), subject to sufficient soil water (25% of soil water capacity)	Leaf growth comes from stored carbon and occurs at a constant rate until the target LAI (50% of the carbon store × specific leaf area) is reached	Leaf drop is triggered when leaves reach their parameterized age (360 days). Small amounts of litterfall occur every day as a function of leaf age	Woodward and Lomas (2004)

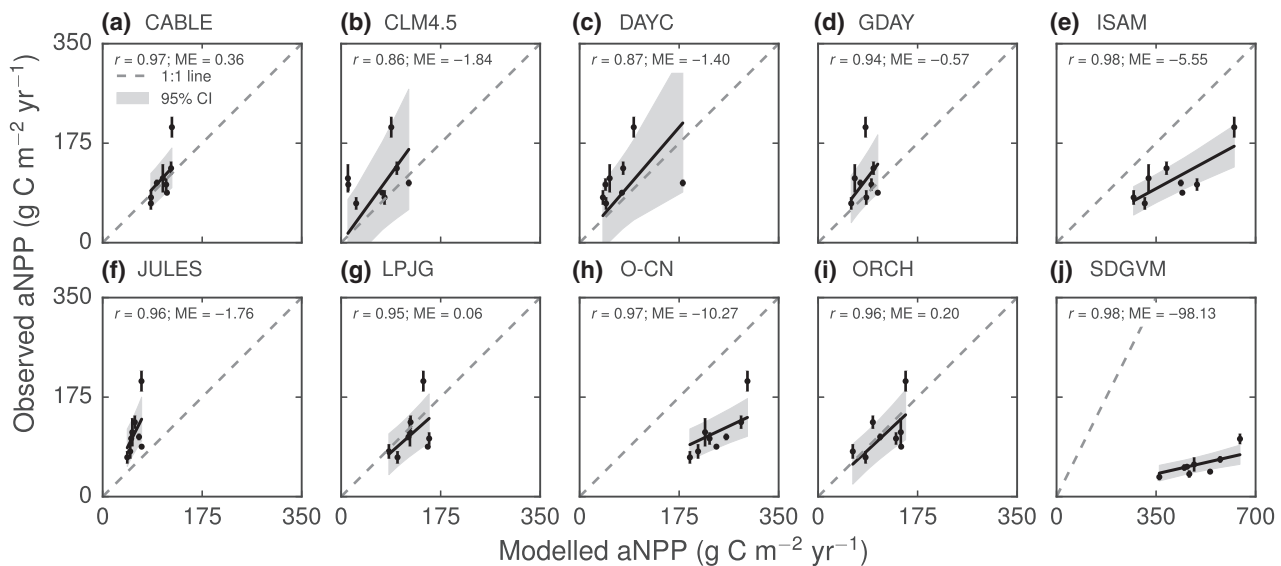


Fig. 2 Scatter plot showing the observed and modelled aNPP in the control (ct) treatment. Vertical error bars (one standard deviation) represent cross plot ($N = 5$) variability in observed aNPP. Note, the SDGVM model (panel j) is shown on a different x-axis range (0–700 vs. 0–350). ME is the Nash–Sutcliffe model efficiency coefficient ($-\infty$ to 1), where 1 would indicate perfect agreement with the observed aNPP. CI is the 95% confidence interval for the modelled values, and r is the correlation coefficient.

observed greenness agree with drops in SWC, particularly in dry years (2007, 2008), but also in a relatively wet year (2011). In wetter years (2009, 2010), greenness and SWC show little correspondence, until sufficient soil drying has occurred to drive a sudden decline in leaf greenness, around day of year (DOY) 200. Inferred vegetation greenness from digital photography does

not directly correspond to leaf area index (LAI), but is well correlated with plant cover and biomass (Zelikova *et al.*, 2015), and so is a reasonable proxy against which to compare modelled LAI. With the exception of CLM4.5, modelled LAI at the site was remarkably smooth both across models and years; none of the models showed the observed strong within-season

Table 2 Causes of differences in modelled aNPP. Values shown are averages across the experiment in the ambient treatment. A_b is the above-ground allocation fraction, CUE is the carbon-use efficiency, GPP_{us} is the unstressed GPP per unit leaf areas, β is the water stress factor, D is the growing season duration, LAI_p is the growing season maximum LAI, $aNPP_c$ is the inferred aNPP which is the product of A_b , CUE, GPP_{us} , β , D/LAI_p , and LAI_p , and $aNPP_a$ is the actual model output for comparison

Model	A_b (-)	CUE (-)	GPP_u (g $C\ m^{-2}\ leaf\ day^{-1}$)	β (-)	LAI_r (day yr^{-1})	LAI_p ($m^2\ m^{-2}$)	$aNPP_c$ (g $C\ m^{-2}\ ground\ yr^{-1}$)	$aNPP_a$ (g $C\ m^{-2}\ ground\ yr^{-1}$)
CABLE	0.13	0.63	8.57	0.33	249.02	1.55	54.33	54.5
CLM5	0.55	0.67	6.27	0.6	155.79	2.99	203.27	197.85
DAYCENT	0.47	0.55	11.92	0.17	126.54	1.29	63.31	64.29
GDAY	0.46	0.5	4.71	0.74	104.07	1.88	82.05	88.16
ISAM	0.85	0.53	5.3	0.82	125.53	2.98	247.15	211.89
JULES	0.82	0.32	3.6	0.2	77.96	1.38	18.86	20.02
LPJ-GUESS	0.31	0.5	4.63	0.77	218.57	2.49	122.1	129.78
O-CN	0.52	0.52	4.81	0.84	169.93	3.08	185.62	246.2
ORCHIDEE	0.47	0.53	3.3	0.97	149.91	1.21	118.13	123.31
SDGVM	0.86	0.69	4.95	0.71	256.11	6.1	542.86	526.82

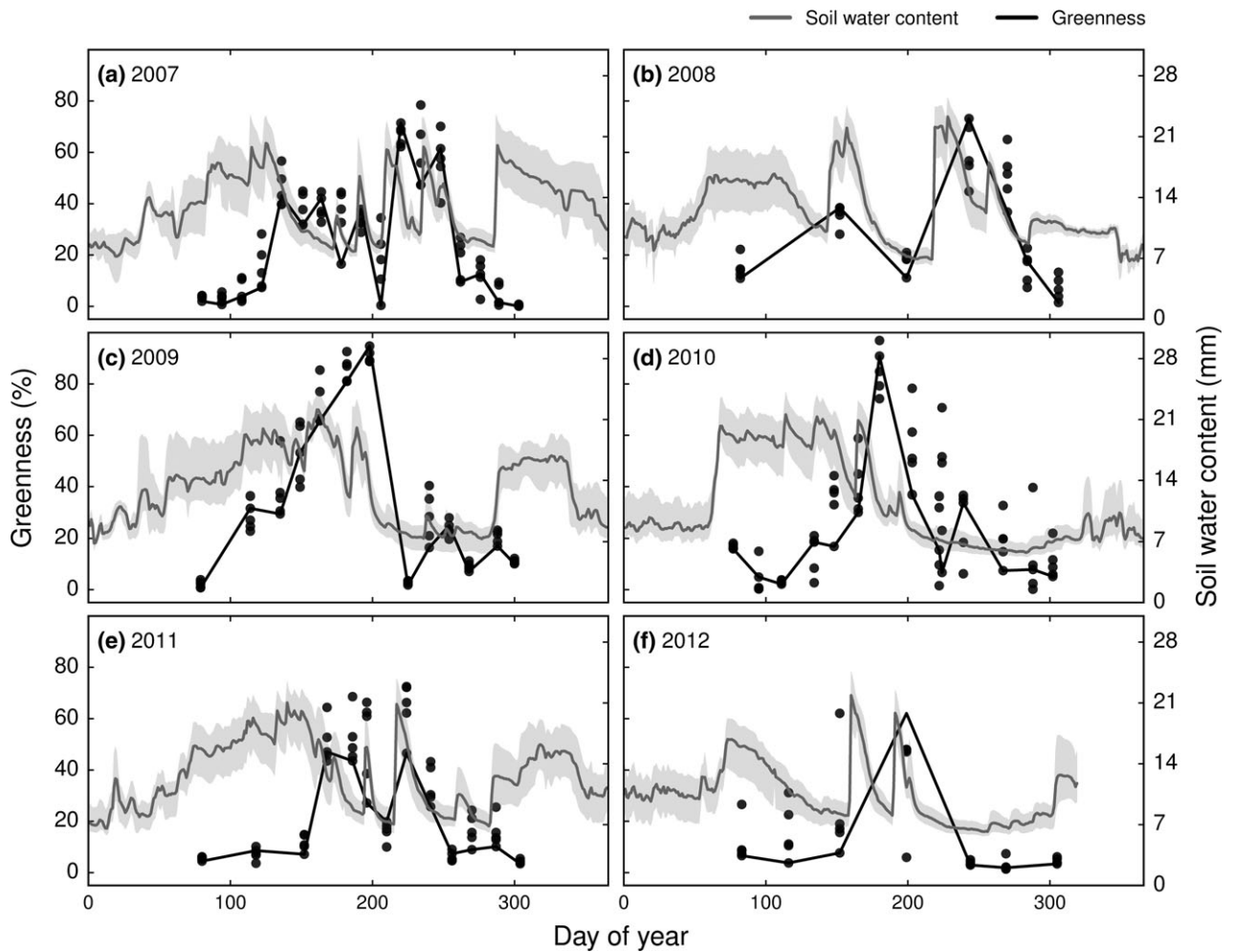


Fig. 3 Greenness (number of green pixels) derived from biweekly digital photographs and the corresponding soil moisture content (top 20 cm) in the ambient plots. Greenness observations are shown with filled black circles, with a fitted spline to aid visual interpretation. Soil moisture data represent the plot means (solid line) and minimum and maximum from the five ambient plots (shaded area).

dynamics seen in the observations (Fig. 4). We conclude that, in general, modelled LAI is insufficiently sensitive to soil water availability in this semi-arid grassland.

The lack of variability within the growing season is a consequence of how models determine growth (Table 1). For deciduous species, DAYCENT and GDAY use the previous year's stored C to grow and in LPJ-GUESS growth is only calculated once at the end of the year, based on the annually integrated NPP. These assumptions introduce a significant lag between growth and meteorology and also result in very smooth growth predictions, because the subannual scale allocation of C is not related to environmental stress. Other

models (CABLE, ISAM) assume specific phenological periods in which growth must occur, and end up with similar smooth phenologies, which are unrelated to environmental conditions. In JULES, O-CN and ORCHIDEE, the current year's growth is directly related to recently fixed C, without assumptions about specific phenological growth stages. Nevertheless, these models display only marginally more within-season variability than the other models. In CLM4.5, C₃ grasses were not able to grow at the site and the extremely variable LAI corresponds to the C₄ grass component.

Table 1 summarizes the key assumptions that dictate modelled leaf emergence and senescence. Both CABLE and SDGVM assume that grasses do not

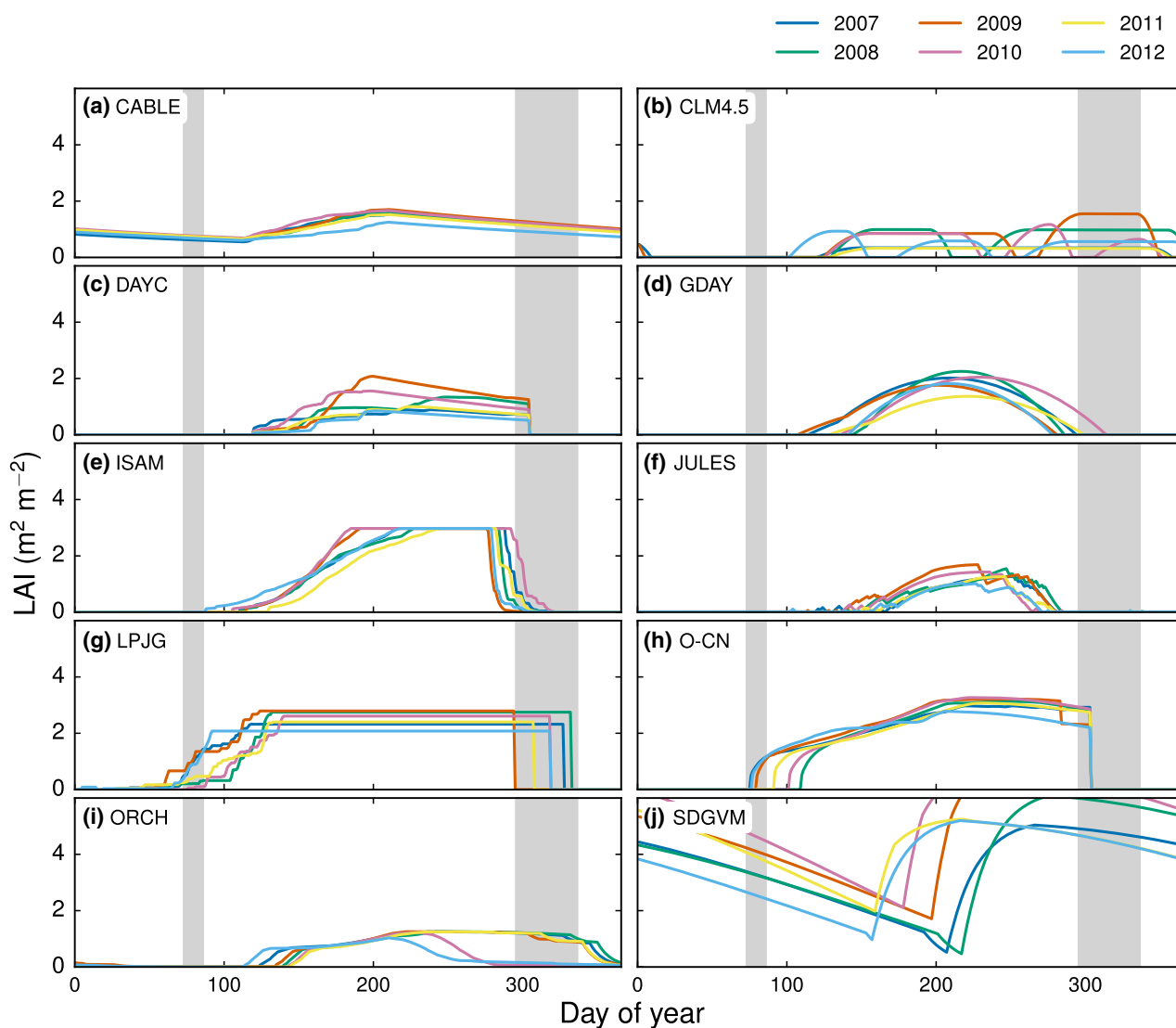


Fig. 4 Modelled leaf area index (LAI) from the ambient (ct) treatment, shown by sequential colours from yellow to dark green, which corresponds to years between 2007 and 2012. Grey shading indicates the range of leaf out and leaf-off dates calculated from the control (ct) treatment (Reyes-Fox *et al.*, 2014).

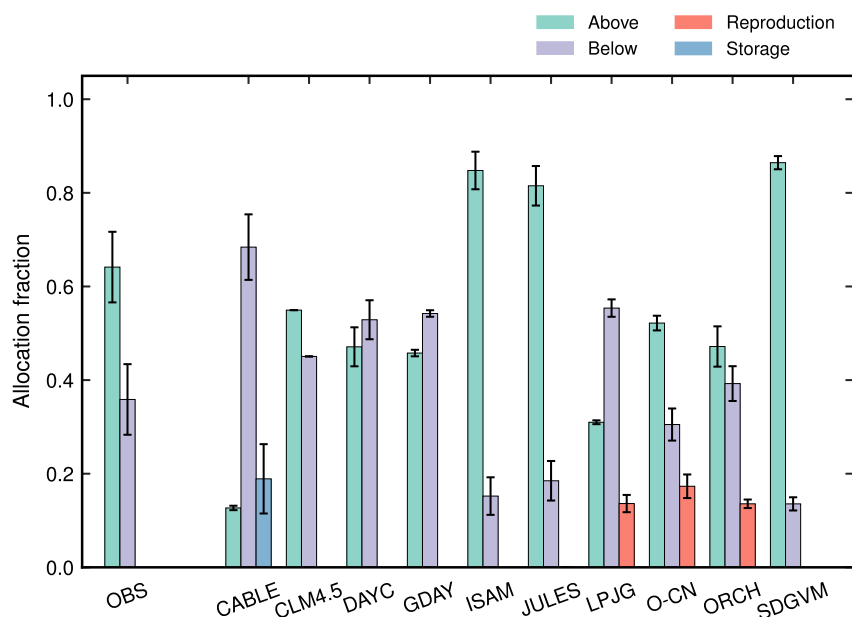


Fig. 5 Fraction of net primary productivity (NPP) allocated above-, below-ground, and to reproduction in the control (ct) treatment.

entirely drop their leaves, behaving instead like dynamic evergreen vegetation. Leaving aside these models (and CLM4.5), most models predicted a later leaf onset date (mean = 40 ± 26 days, 1 standard deviation) than was observed at the site. LPJ-GUESS was the exception, predicting an earlier leaf onset, mean ~ 11 days.

Conversely, modelled leaf senescence typically occurred at or after DOY 300, which meant models were broadly consistent with the range in leaf drop dates observed at the site (Reyes-Fox *et al.*, 2014). Despite this seemingly better agreement with observed leaf senescence, the data in Fig. 2 suggest that while the grasses maintained standing biomass, these leaves were no longer productive. Towards the end of the growing season, there is a drop in vegetation greenness, which signifies a change in leaf chlorophyll content. By contrast, the models assume that as long as there is leaf area, sufficient soil water and radiation, leaves are actively photosynthesizing. This group of models does not explicitly simulate the grass curing process (i.e. the transition from green to brown standing leaves). Thus, the models typically overestimated the period that leaves were photosynthetically active by ~ 50 – 100 days, even in wet years.

Carbon allocation (A_b)

Models predict LAI as a consequence of allocation of net primary productivity (NPP) and stored carbohydrates to leaves, the subsequent turnover of these

tissues, and assumptions about specific leaf area. We inferred observed above- and below-ground allocation fractions from biomass data and an assumed fine-root lifespan of 5.8 years (Fig. 5). This estimate is based on root growth and disappearance in minirhizotron images from a nearby study (Milchunas *et al.*, 2005) and is consistent with an isotope-based estimate of carbon in the roots of 6–7 years at the site (Carrillo *et al.*, 2014). No treatment effects were found on root turnover in either study. As there is uncertainty about this estimated lifespan, we also show these data as above- and below-ground ratio (Fig. S1). Site data suggested that the proportion of NPP allocated above-ground (64%) was greater than belowground (35%). Models strongly disagreed about the proportion of C allocated above vs. below-ground, and no model agreed with the observations. At the extremes, CABLE predicted that $\sim 70\%$ of C was sent below-ground, while ISAM, JULES and SDGVM predicted $>80\%$ was allocated above-ground (Fig. 5). Much of the detail as to why these models disagree in terms of allocation has been documented previously (De Kauwe *et al.*, 2014). In agreement with these earlier findings, models (GDAY, LPJ-GUESS, O-CN, ORCHIDEE) that implemented a functional balance (between leaves and roots) predicted more balanced allocation fractions. Among these models, higher allocation below-ground (CABLE, GDAY, LPJ-GUESS) indicated greater N and/or water stress. This prediction was also in line with the DAYCENT model, which allocates C to the plant tissue with the greatest resource limitation.

Sensitivity of productivity to soil moisture (β)

Another key explanation for model differences was related to soil water content (SWC). Models were parameterized with the same soil water-holding capacity, so differences in predicted SWC partly relate to differences in LAI (Fig. 3), but also to soil evaporation. Models disagreed on both the available SWC, as well as the sensitivity of productivity to SWC. Figure 6 shows modelled soil water time series in a dry (2008) and a wet year (2009). Despite differences in the absolute SWC, with the exception of CABLE and ISAM, most models predicted consistent declines in SWC, with earlier declines in the dry year. ORCHIDEE (mean = 44 mm yr⁻¹), SDGVM (mean = 62 mm yr⁻¹), O-CN (mean = 81 mm yr⁻¹) and LPJ-GUESS (mean = 129 mm yr⁻¹) predicted comparatively low total soil evaporation fluxes across years, whereas the

other models predicted ~2–3.5 times greater annual evaporative fluxes. The SDGVM result is likely explained by continuous (and high) foliage cover, but this does not apply to the other models which simulate lower LAI. In a semi-arid system, these variations among models in predicted water losses are concerning.

Models also strongly disagreed on the level of water stress, shown by the growing season simulated water stress factor (β ; water stress factor which limits productivity as water content declines), which is used to limit gas exchange as water availability declines (Fig. 7). β varied markedly between models. For some models (DAYCENT, JULES, LPJ-GUESS), there is no obvious distinction between wet and dry years. This variation is caused by different assumptions among the models as to the shape of the functions used to represent the effect of water stress (Medlyn *et al.*, 2016; Fig. S2). Notably,

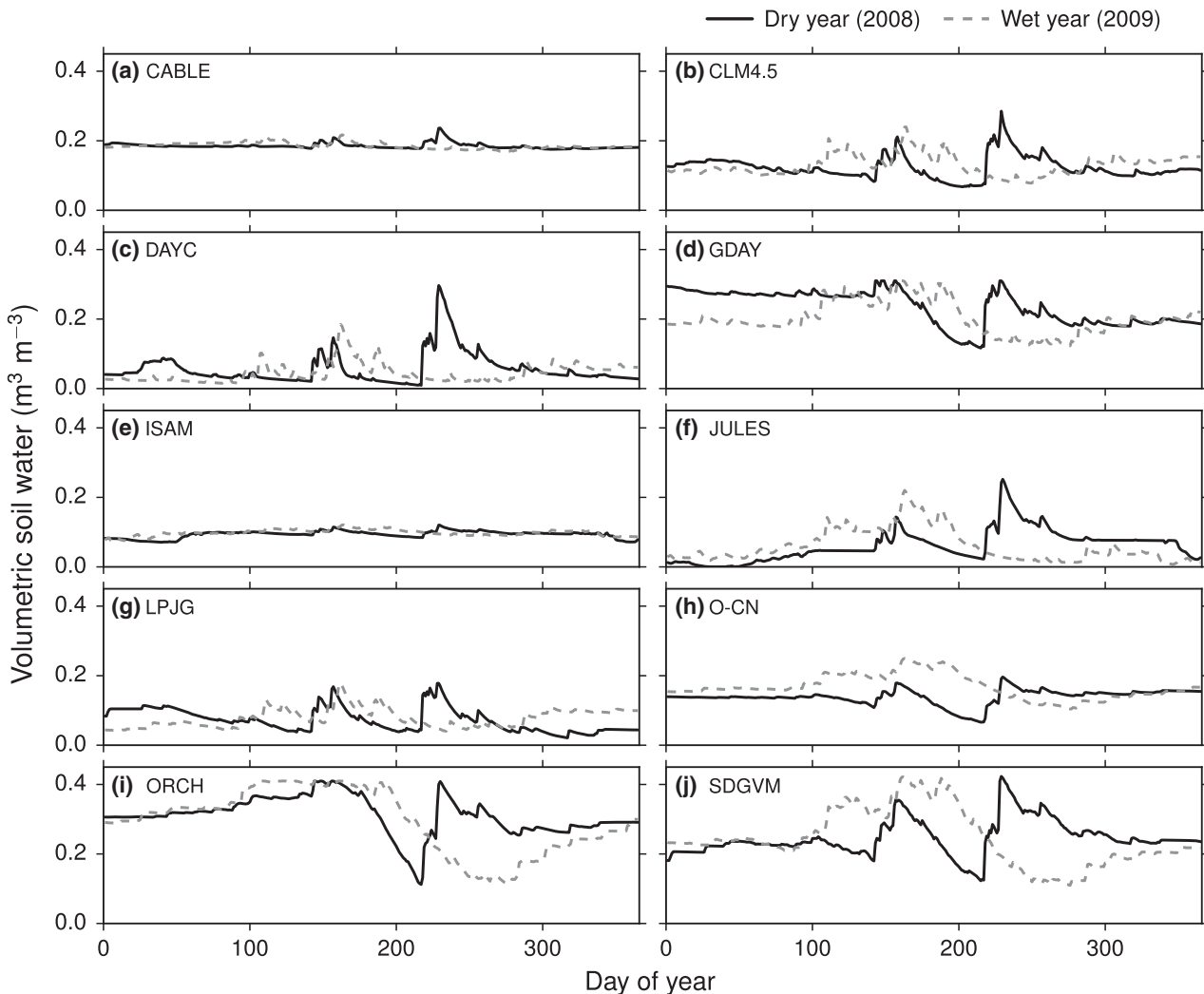


Fig. 6 Modelled soil water profile in a dry (2008) and a wet year (2009).

ORCHIDEE predicted no stress because in this version of the model (IPCC's Fifth Assessment version), the hydrological cycle is represented by a two buckets layer scheme. Using this representation, drainage or surface run-off occurs only when both buckets are full. Therefore, this scheme generally underestimates run-off and consequently overestimates the soil water content and underestimates the soil water stress for plants.

Response to CO₂

We assessed modelled responses to eCO₂ by comparing results against measured above- and below-ground

biomass data. We also explored modelled responses of N mineralization, uptake and changes in N use efficiency, comparing results to summary data from the site.

To understand model predictions, we split above-ground response into C₃ and C₄ components. Figure 8 shows marked year-to-year variability in the observed aNPP responses to CO₂ in C₃ species: observed aNPP responses were between 11% and 39%, averaging 16%. In 2009 (the wettest year), the observations showed a 6% decrease in aNPP because the ambient plots were more productive than the eCO₂ treatment plots. The modelled CO₂ effect on

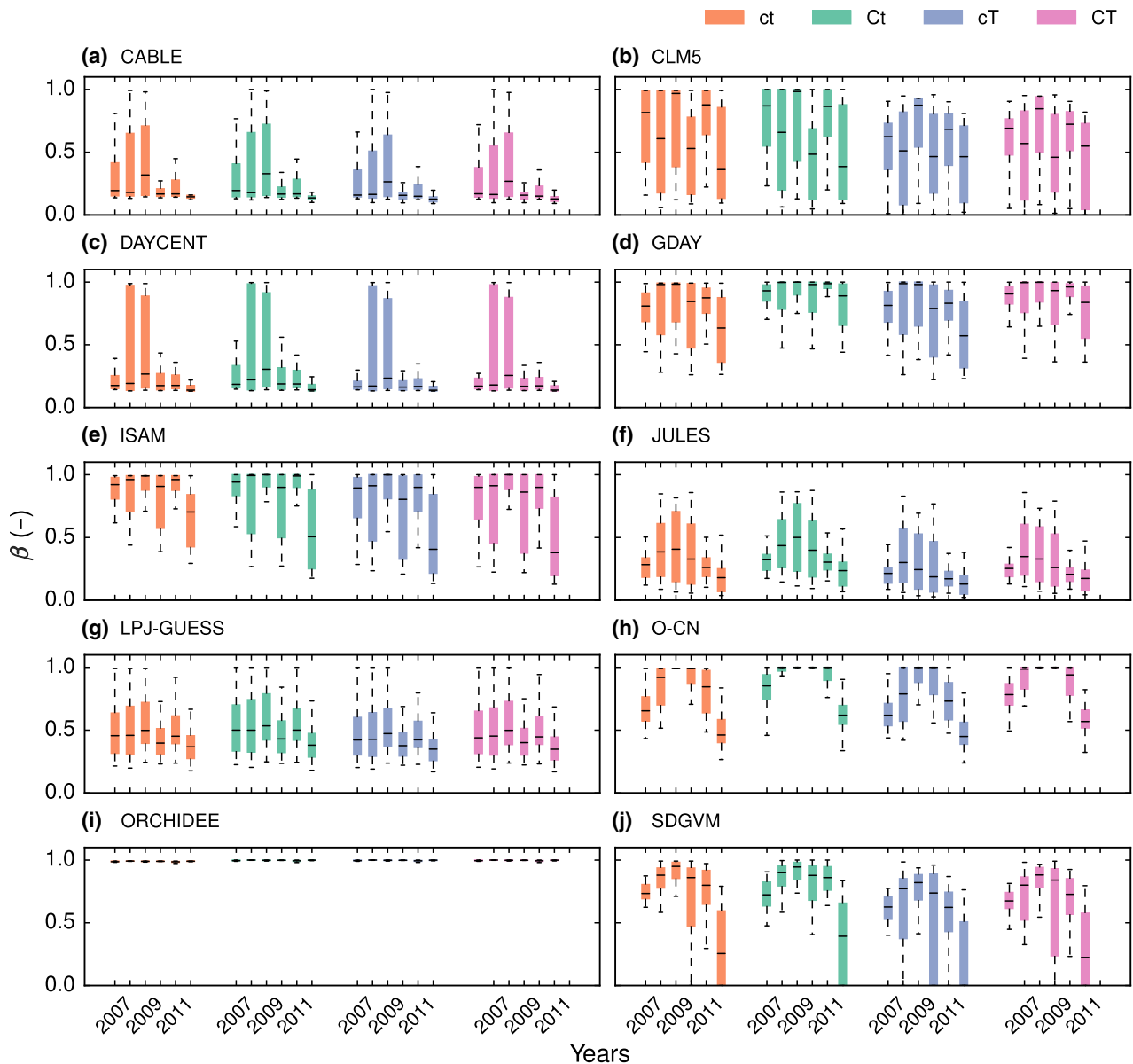


Fig. 7 Summer (June, July, August) soil water availability factor (β) in the control (ct), CO₂ (Ct), warming (cT), and CO₂ × warming (CT) treatments. Error bars show summer interannual variability across the experimental years.

aNPP averaged 29% (range: -12 to 63%). However, with the exceptions of CABLE and ISAM, model responses were within the range of the observed treatment responses in most years when considering standard errors calculated across replicates. While models seemingly appear unable to capture the inter-annual variability of the enhancement due to CO₂, the uncertainty on the observed responses is large, meaning most of the simulated responses are plausible.

Observed aNPP responses to CO₂ for C₄ species were negative for 4 of the 6 years, with aNPP on average

decreasing by -4%. The models predicted more modest changes in aNPP, mean = 5% increase, range: -27 to 16% (Fig. 9), which is within the range of observed responses including the standard errors of treatment replicates.

The change in aNPP in response to CO₂ is itself a result of changes in GPP, autotrophic respiration, and allocation. To investigate these changes, we separated these average responses for each component for C₃ (Table 3) and C₄ (Table 4) species. We focus on differences in the responses of C₃ species as this is where the models disagreed most. We examine the change in

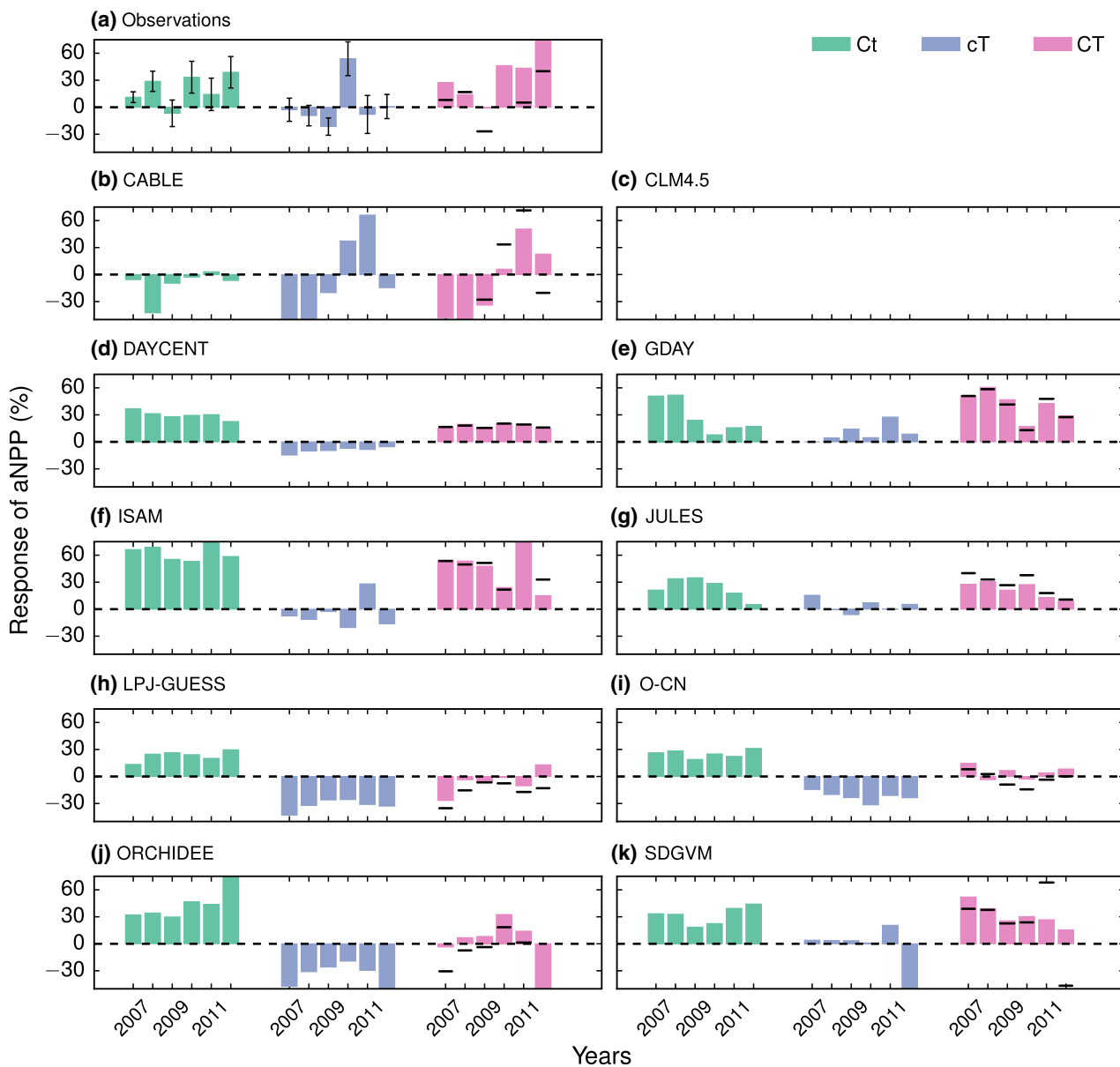


Fig. 8 Response of aNPP to CO₂ (Ct), warming (cT), and CO₂ × warming (CT) for C₃ species. Error bars on the Ct and cT observed treatments denote one standard error. Horizontal lines on the CT treatment bars show the estimated interactive terms if this interaction was additive.

autotrophic respiration by looking at the CUE, or the fraction of GPP not respired.

Most models predicted an increase in GPP in response to eCO₂, with the mean annual increase ranging between 30 and 73%. JULES predicted the largest GPP response to CO₂ (mean = 73%) and CABLE the smallest (mean = 21%). The direct effect of CO₂ on leaf-scale photosynthesis should theoretically be on the order of 25–30% (Franks *et al.*, 2013) for the treatment change in CO₂ concentration. In the models, the predicted effect is greater because of indirect feedbacks through increased soil moisture and LAI.

Among the C-cycle only models (JULES, ORCHIDEE, SDGVM), the mean annual response of GPP to CO₂ varied strongly (range: 31–73%). JULES had the largest stimulation because under ambient conditions, the model is particularly water stressed (Fig. 7), and eCO₂ alleviates this water stress, which results in large CO₂ stimulation of GPP. ORCHIDEE and SDGVM predicted similar mean values (different interannual variability), but for different reasons. At ambient CO₂, ORCHIDEE did not predict any water stress, and as a result, the benefit of CO₂ via water savings was negligible. In SDGVM, the GPP response to CO₂ was low due to the

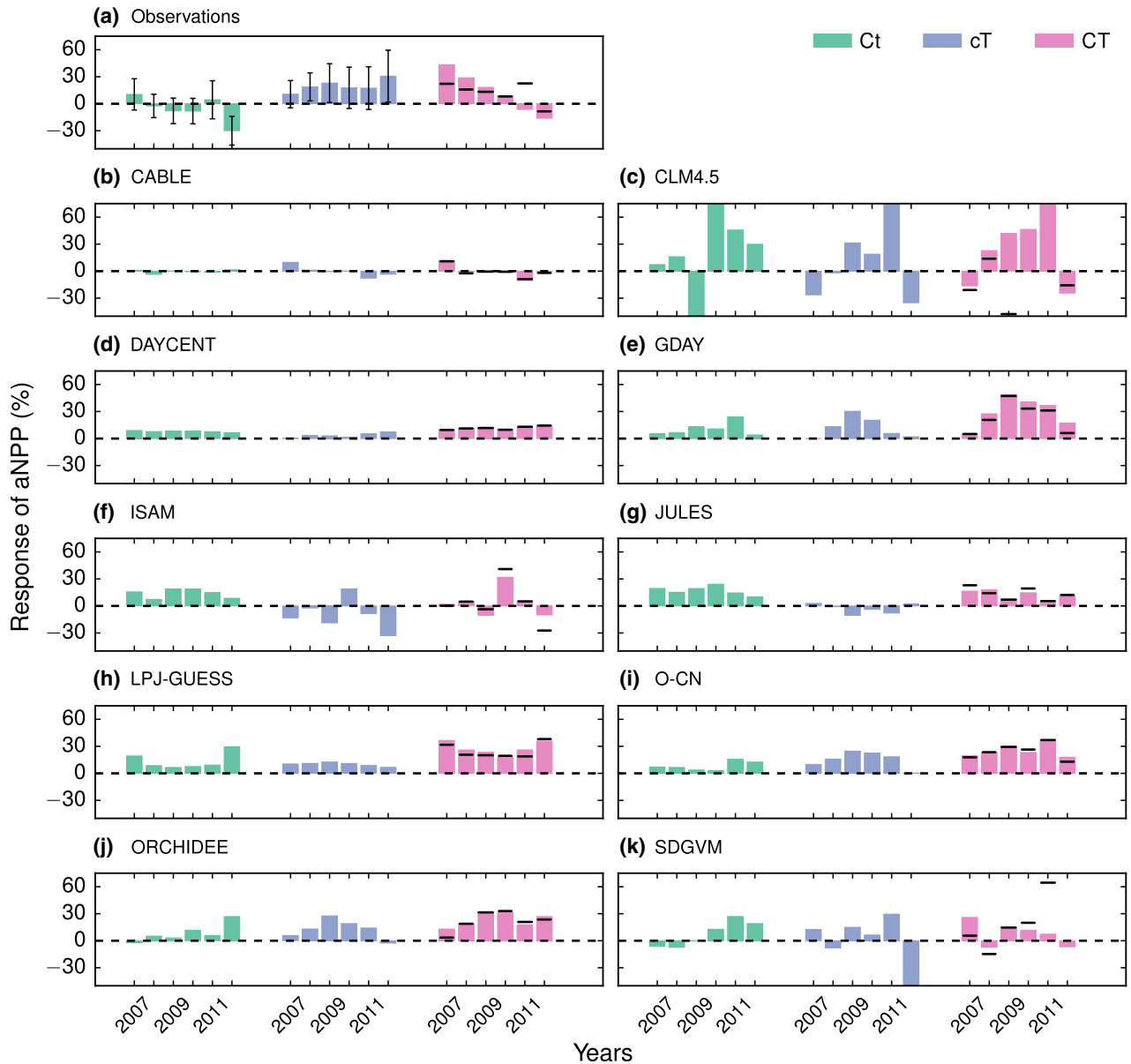


Fig. 9 Response of aNPP to CO₂ (Ct), warming (cT), and CO₂ × warming (CT) for C₄ species. Error bars on the Ct and cT observed treatments denote one standard error. Horizontal lines on the CT treatment bars show the estimated interactive terms if this interaction was additive.

Table 3 Causes of differences in the modelled aNPP response to CO₂ for C₃ species. Values shown are averages across all years. GPP is enhancement expressed as a percentage, CUE is the carbon-use efficiency, expressed as a percentage, A_b is the percentage change above-ground allocation, B_g is the percentage change below-ground allocation, and S is the percentage change in allocation to labile carbon storage

Model	GPP (%)	CUE (%)	A _b (%)	B _g (%)	S (%)
CABLE	20.65	2.86	-4.13	-11.02	15.15
CLM5	-	-	-	-	-
DAYCENT	45.45	-12.2	0.72	-0.72	0
GDAY	39.13	0	-4.55	4.55	0
ISAM	55.13	-3.07	3.74	-3.74	0
JULES	72.62	5.06	-3.57	3.57	0
LPJ-GUESS	15.44	16.62	0.64	-0.64	0
O-CN	53.66	-11.32	2.41	-2.41	0
ORCHIDEE	31.21	4.92	1.59	-1.59	0
SDGVM	33.45	-2.05	-1.73	1.73	0

Table 4 Causes of differences in the modelled aNPP response to CO₂ for C₄ species. Values shown are averages across all years. GPP is enhancement expressed as a percentage, CUE is the carbon-use efficiency, expressed as a percentage, A_b is the percentage change above-ground allocation, B_g is the percentage change below-ground allocation, and S is the percentage change in allocation to labile carbon storage

Model	GPP (%)	CUE (%)	A _b (%)	B _g (%)	S (%)
CABLE	22.42	2.98	-2.42	-11.47	13.89
CLM5	19.1	-1.72	0	0	0
DAYCENT	12.58	-4.53	0.17	-0.17	0
GDAY	16.85	0	-0.99	0.99	0
ISAM	9.43	2.7	-0.3	0.3	0
JULES	34.51	6.89	-0.87	0.87	0
LPJ-GUESS	26.37	4.69	-1.95	1.95	0
O-CN	6.8	-0.08	2.34	-2.34	0
ORCHIDEE	4.75	0.64	1.57	-1.57	0
SDGVM	10.15	-2.73	-2.38	2.38	0

high ambient LAI (Fig. 4), which meant that canopy photosynthesis was primarily light-limited. In addition, this high LAI meant that there were negligible benefits to be gained from CO₂ induced water savings, due to high transpiration.

GPP responses among the N cycle models were also not consistent (mean range: 20 to 55%), particularly evident in the year-to-year variability in the size of the enhancement. There was pronounced variability in modelled N availability due to different levels of productivity (see Fig. 2) during model spin-up. Models could be categorized into three groups: at the low end, the mean inorganic N pool was between ~0.3 and 1.3 g N m⁻² (CABLE, GDAY, LPJ-GUESS and O-CN),

in the middle ~30 g N m⁻² (CLM5, ISAM), and at the high end 177 g N m⁻² (DAYCENT). Site soil N measurements suggested an inorganic pool size (0.4 g N m⁻²) towards the lower end of the model predictions (Dijkstra *et al.*, 2012). Most models (CABLE, DAYCENT, GDAY, LPJ-GUESS) predicted large increases (>20%) in photosynthetic N use efficiency (GPP/canopy N; PSNUE; Fig. S3). CLM4.5, ISAM, and O-CN predicted large increases (>20%) in N uptake (Fig. S4), which combined with increased N mineralization (Fig. S5) in ISAM and O-CN, resulted in sustained GPP responses to CO₂ in these models. CABLE also predicted a reduction in N losses in response to CO₂, but this change was small (~0.3 g N m⁻²) when integrated across the experiment and thus, made a negligible difference to total N availability. N losses were thought to have been low for the site (Dijkstra *et al.*, 2010).

The modelled increases in N mineralization (Fig. S5) in response to CO₂, particularly in the ISAM and O-CN models, were at odds with the site data. Although there is no direct site evidence of N limitation, Dijkstra *et al.* (2012) showed evidence of dilution in plant N concentrations with increasing soil water, which would suggest plant N demand increased by more than the net N mineralization rate. The increased N mineralization in O-CN was caused by decreased soil organic matter, whereas in ISAM, it was driven by the increased C:N ratio of the soil organic matter. Generally, these models did not predict the increased microbial N immobilization because inorganic N pools were sufficiently saturated. Had these models started with smaller inorganic N pools (similar to that used by GDAY), then the changes in N availability in response to treatment would also have been smaller and more in line with what was observed. Models that implement a variation of the CENTURY soil model have the mechanism to predict the observed sites changes in N availability and ultimately the differences come down to the availability of N, which differed due to different end states after model spin-up.

We now examine the contribution of changes in CUE to the aNPP enhancement (Tables 3 and 4). Most models predicted modest changes although models disagreed on whether total respiration increased or decreased with CO₂ (-12 to 14%). The DAYCENT and O-CN models assume that nutrient limitation results in excess C being respired, which results in a decreased CUE at eCO₂.

Changes in allocation in response to CO₂ were low across all models, typically of the order of ± 5% (Tables 3 and 4). CABLE predicted ~15% increase in the NPP allocated to the labile storage pool in both C₃ and C₄ plants, which occurs because in CABLE plants were unable to acquire sufficient N to grow tissues. This N

limitation largely explains the negative response (mean = 12%) of aNPP to CO₂ despite the GPP enhancement (mean = 21%). CABLE simulated a very large labile C store: the elevated mean was 3983 g C m⁻² yr⁻¹ at eCO₂ compared to ambient, mean = 708 g C m⁻² yr⁻¹.

The explanation as to why the high GPP response to CO₂ (73% enhancement for C₃ species) only resulted in a more modest increase in aNPP in JULES relates to the C allocated for competition (termed 'spreading' in JULES). In this study, competition was switched off, and as a result, the additional C fixed by the plant in response to CO₂ was largely allocated to this competition process and so was not actually available to the plant to grow.

Shifting focus to changes in phenology, one of the principal results of the experiment, was that eCO₂ resulted in a longer growing season in 3 of the 5 years (Reyes-Fox *et al.*, 2014). In 2009, the last species to reach senescence did so 15.6 days later than in the ambient conditions. However, in other years, the change was smaller, 3.2 and 1.5 days in 2008 and 2011, respectively (Reyes-Fox *et al.*, 2014). Notably, in 2007 (9.8 days) and 2010 (3.6 days), senescence was actually earlier, shortening the growing season. These results complicate drawing concrete conclusions about the effect of CO₂ treatment given the large interannual variability, which was mediated by precipitation and soil moisture (Zelikova *et al.*, 2015).

Tables S1 and S2 show the change in growing season length in response to treatment in the models. Leaf senescence was only delayed in the ISAM (0.8 days, range = -5 to 5 days) model; however, this response did not relate to a CO₂ effect on soil water, but instead was an outcome of the use of phenological phases. The senescence phase occurs only when LAI declines to 95% of a prescribed upper threshold. eCO₂ results in an increase in LAI, and therefore, LAI does not fall below this threshold, which lengthens the growing season (see De Kauwe *et al.* (2014) for details). A number of models determine their leaf drop dates (Table 1) based solely on air temperature (GDAY, JULES) and so miss any positive effect of any CO₂ induced soil water savings on growth via changes in leaf senescence. Other models (LPJ-GUESS, ORCHIDEE, O-CN; see Table 1) do consider a minimum soil water status when determining leaf drop, but soil water savings were not great enough to maintain the water status above these thresholds.

Observed root biomass was increased on average by 11% with CO₂ treatment (Fig. 10). With the exception of SDGVM, the models broadly enveloped the size of the observed increase, mean range: 7–17%. However, models did not capture the year-to-year variability.

Increased N stress throughout the course of the experiment led to a greater allocation to roots in GDAY, LPJ-GUESS and O-CN, as they simulate N uptake as a function of root biomass and allow allocation to shift in response to resource availability. By contrast, DAYCENT predicted a very small increase, because at ambient CO₂ fine-root allocation was already high (Fig. 4), which meant allocation to leaves was prioritized under eCO₂. SDGVM follows a leaf optimization scheme for C allocation. Responses of allocation to leaves and roots in SDGVM largely matched the responses of GPP to CO₂, as grass allocation uses fixed fractions (Table 1), which explains the large mean enhancement of 38%.

Response to warming

Observed aNPP of C₃ species only increased in response to warming in 2011 (+53%); in all other years, the warming treatment had a negative effect. However, of all the five years which had negative responses, only one did not also include the potential for a positive treatment response once we accounted for the standard error of treatment replicates. CABLE apart, the models generally predicted a small response of aNPP to warming, although the direction of the treatment effect varied among models, plant functional groups and across years (Figs 8 and 9). Among the N cycle models, the balance between the warming-induced treatment increases in N mineralization (Fig. S5) and decreases in soil water (Fig. 7) explained interannual variability in aNPP responses. Warming particularly enhanced N mineralization in GDAY and LPJ-GUESS. For C₃ species, soil water stress also increased (Fig. 7), which limited responses (less mineralization) in the O-CN and DAYCENT models. Similarly, among the C-cycle models (JULES, SDGVM), the warming treatment increased water stress, which reduced the aNPP response.

Warming consistently led to an earlier leaf expansion in the observations, mean = 5.1 days (range 0.9–9.6 days; Reyes-Fox *et al.*, 2014). The effect on leaf senescence was mixed: shortening the growing season in 2007 (3.3 days) and 2009 (6.9 days) and lengthening it in other years, 3.3, 0.4, and 8.5 days in 2008, 2010, and 2011, respectively. Most models did predict an earlier spring growth in response to warming, as warmer temperatures meant that models passed their assumed growing degree-days threshold earlier (see Table 1). However, the magnitude of the change was considerably larger than observed: on average by 15.9 days (range 2–24.3 days). Three of the models (CABLE, DAYCENT, SDGVM) predicted no change. In DAYCENT, the warming effect on leaf-on/off dates was prescribed, so it does not capture a treatment effect. In CABLE and SDGVM, LAI is assumed not to reach

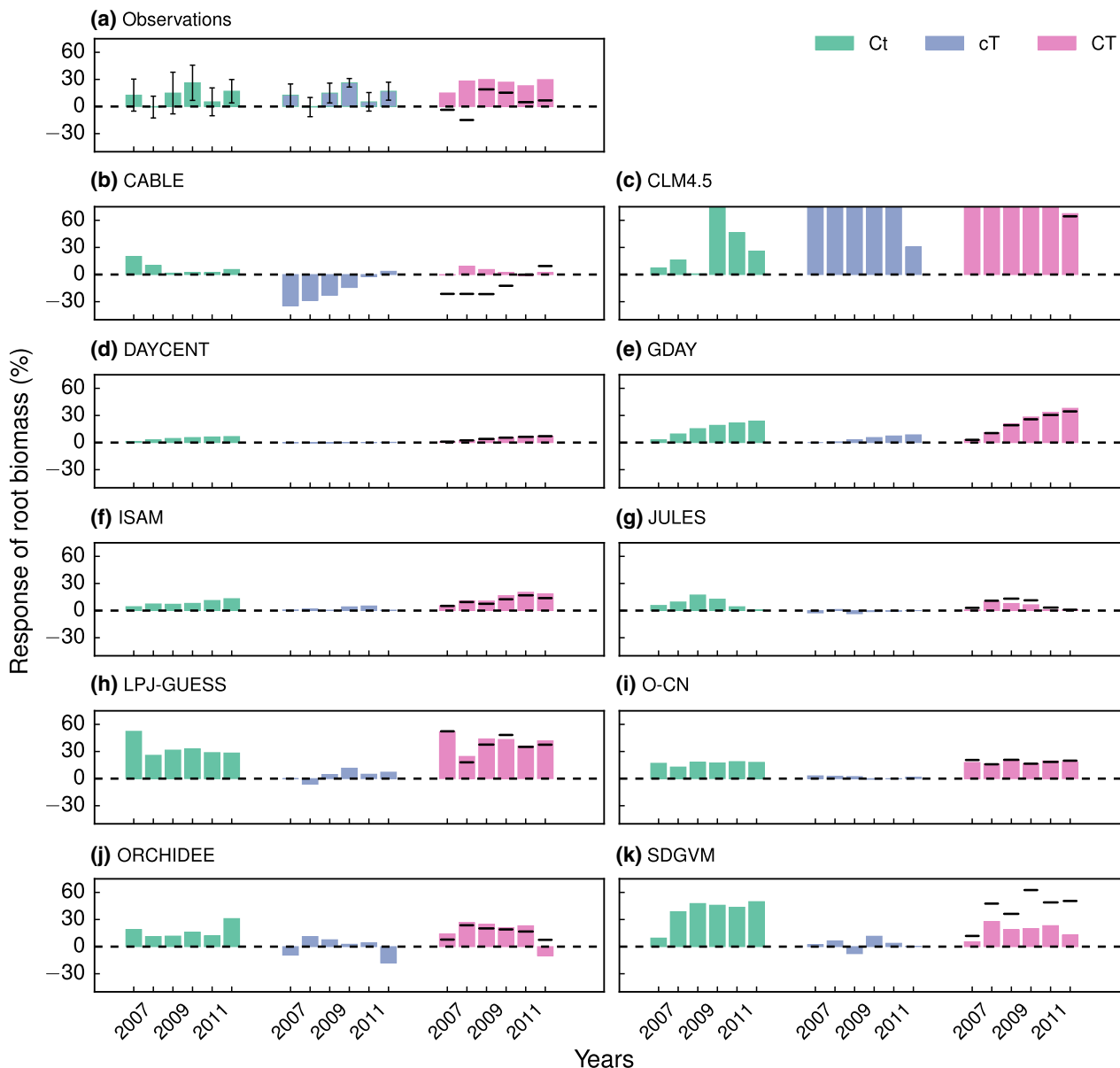


Fig. 10 Response of root biomass to CO₂ (Ct), warming (cT), and CO₂ × warming (CT). Error bars on the Ct and cT observed treatments denote one standard error. Horizontal lines on the CT treatment bars show the estimated interactive terms if this interaction was additive.

zero (see above). Finally, in two of the years, LPJ-GUESS predicted a delayed leaf onset (11 and 38 days) with warming, which was a result of limited soil water availability. The trigger for growth in LPJ-GUESS is simply air temperature, which means the model attempted to grow very early in some years (e.g. DOY 12 in 2010), but development is temporarily shut off when soil water is below a threshold level. In the warming treatment, warmer temperatures led to increased soil water depletion (via soil evaporation), which had the effect of delaying leaf onset. Nevertheless, in years where soil water stores were greater

(2008), the direction of change in response to treatment matched the other models (not shown).

The small changes in root biomass in response to warming among the models follows the small aNPP response (Fig. 7) and, as with the response to CO₂, models again enveloped the observed change (Fig. 10).

CO₂ × warming

To examine the interactive effect, we calculated the observed additive response to CO₂ × warming treatment for C₃ aNPP (Fig. 8), C₄ aNPP (Fig. 9), and root

biomass (Fig. 10), shown by the black horizontal lines. Observations generally show greater than additive interactions in both above- and below-ground biomass. DAYCENT is the only model to predict additive responses to the combined treatment. Models do not predict consistent interactions: responses are just less than additive, additive, or considerably greater than additive. Models that predict greater than additive interactions do so as a result of a positive effect of warming on N mineralization (Fig. S5), combined with increased CO₂-induced water savings (Fig. 7).

In the observations from combined treatment plots, leaf expansion was earlier than in the ambient treatment, mean = 4.6 days (range 2.4–7 days), but the effect was smaller than in the warmed plots (Reyes-Fox *et al.*, 2014). There was a clear interaction on the leaf drop dates: the combined treatment resulted in an increased growing season length of 22.4 days in 2009 (Ct = 15.6 days), despite the warming treatment shortening the growing season by 6.9 days. Across all years, the response to the combined treatment was consistent, increasing the growing season length mean = 7.9 days (range 0.1–22.4 days; Reyes-Fox *et al.*, 2014). With the exception of ISAM (not related to treatment, see above), the models did not predict the observed interaction between eCO₂ and warming on phenology.

Discussion

Evaluating models against ecosystem-scale manipulation experiments has the potential to produce significant insight into model performance (De Kauwe *et al.*, 2013; De Kauwe *et al.*, 2014; Zaehle *et al.*, 2014; Medlyn *et al.*, 2015; Walker *et al.*, 2015).

Our intercomparison has identified a number of important model failings. Several of these have been identified in previous model comparisons against FACE experiments, such as C allocation (De Kauwe *et al.*, 2014); flexibility of plant stoichiometry (Zaehle *et al.*, 2014); and sensitivity to drought stress (Medlyn *et al.*, 2016). There are, however, a number of new issues identified in this study, namely grassland phenology; link between soil water stress and growth; soil N availability; interannual variability; and C storage/grassland physiognomy.

Soil water stress

In semi-arid ecosystems, water availability is a key determinant on productivity. The wide disagreement in the level of water stress among models (Fig. 6) is alarming, particularly given the models were all initialized with the same effective soil water bucket size.

Differences in level of water stress among models drove differences in modelled productivity both in ambient conditions and in response to treatments, particularly warming. There were two main causes for these differences among the models: a large difference in simulated soil evaporation and differences in sensitivity of productivity to water availability (Figs 7 and S2).

The issue of different modelling schemes simulating sizeable differences in soil evaporation is not a new one (see Desborough *et al.*, 1996). Nevertheless, in water limited systems, it is the principal control on early-growing season water in the root zone. Data from existing eddy covariance towers located at grassland sites should offer a strong constraint on modelled soil evaporation fluxes.

Medlyn *et al.* (2016) recently questioned the empirical support for a number of the functions used by the models in this study. There is therefore a clear need for models to implement more evidence-based functions for the representation of drought stress (De Kauwe *et al.*, 2015). Considerable research is now being targeted to address this need (Zhou *et al.*, 2013, 2014; Verhoef & Egea, 2014). One issue is that many ecosystem manipulation experiments only measured SWC in part of the root-zone profile, as at PHACE where SWC was measured to 25 cm depth (D. M. Blumenthal, in prep). To quantify sensitivity to SWC, time courses of SWC throughout the entire root zone are required, along with information on rooting distributions and regular gas-exchange measurements (e.g. Pendall *et al.*, 2013).

Grassland phenology

Models struggled to replicate the grassland phenology dynamics, both under ambient conditions and in response to climate change treatments. With the exception of the CLM4.5 phenology scheme, most models predicted the growing season length in line with the observed, but this blanket statement ignores some notable gross errors. A number of the models were late in predicting the start of the growing season, often by as much as a month, because they overestimated the temperature required to initiate growth in this cold-temperate grassland. The models that determine leaf senescence based solely on the ambient temperature did not predict the observed CO₂ effect on soil water that maintained growth in some years (Reyes-Fox *et al.*, 2014). Two of the models (CABLE, SDGVM) do not simulate true deciduous behaviour. These failures suggest that the triggers for growth and senescence in these models need to be re-examined.

In this ecosystem, vegetation greenness (a proxy for LAI) was highly dynamic in response to soil water

availability (Fig. 2). The models, in contrast, are not as responsive to soil water availability and do not depict a clear threshold change in greenness with water stress. There is a clear need to improve our quantitative understanding of the mechanisms that determine the water-related dynamics of canopy greenness and senescence in grassland ecosystems.

There has been considerable work done on applying model-data fusion techniques to satellite-derived estimates of LAI, fractional cover, and, more recently, PhenoCams to improve predictions of LAI (Richardson *et al.*, 2009; Knorr *et al.*, 2010; Migliavacca *et al.*, 2011). For example, Hufkens *et al.* (2016) optimized a model to PhenoCam data from 14 North American grassland sites and demonstrated that a single parameterization was able to capture the dynamics of changes in grassland fractional cover. Models could look to these studies to determine parameters constrained by data for their phenology models. However, Hufkens *et al.* (2016) did not consider the effect of eCO₂. Our results show that the models are not able to currently translate any CO₂-induced soil water savings into extended growing seasons, which has obvious consequences for predicting responses to future global change. In models that do account for soil water status when determining leaf drop (O-CN, ORCHIDEE, LPJ-GUESS), the threshold is arbitrarily defined. Phenology data sets from manipulative experiments, along with measurements of soil water status, could be used to inform this key process using similar data-model fusion approaches.

A further reason for the smooth phenology simulated by models relate to the use of a long-term carbon storage pool. This pool effectively dampens day-to-day dynamics, and while a desirable process, the models currently lack fundamental controls on growth (e.g. meristems) which are independent of carbon fixed through photosynthesis. The models are also unable to rapidly shift allocation patterns between pools in response to changing environmental conditions, such as allowing browning in dry conditions.

A related issue is the lack of crown biomass data. Crown biomass is a key ecosystem component, acting as the principal store of reserve carbohydrates in grassland ecosystems; however, it is difficult to quantify. Estimated values during the experiment ranged from <50–500 g m⁻² and in the 2013 final harvest averaged 260 g m⁻² (L. Neslon, in prep). Data used in this study did not account for the crown biomass component, which may have biased inferred allocation fractions. Assuming that including crown biomass would have doubled root-biomass estimates, the below- vs. above-ground allocation would be considerably increased (0.52:0.48), compared to results presented in Fig. 5 (0.36:0.64).

Available nitrogen

Among the N cycle models, a key cause of disagreement was the simulated size of the available N pools at the start of the experiment. This issue was raised previously (Zaehle *et al.*, 2014), but the impact of model predictions is more apparent in this intercomparison. Key differences in how the N cycle is implemented, including the processes that govern the amount of N fixation, the flexibility of plant stoichiometry, and the ability of the models to increase N uptake, affect the initial N stocks through model spin-up and during the course of the manipulation experiment. To constrain these differences among the models would require a more complete observational record of both the N site history and the N budget. While there were site measurements of plant C, N, P ratios (Dijkstra *et al.*, 2012; Mueller *et al.*, 2016), these data are not sufficient to constrain a number of the key disagreements in the change in N dynamics simulated in this study. Experimental measurements of N mineralization rates, N uptake, nitrification/denitrification rates, and biological N fixation would greatly help to better constrain model uncertainties.

Interannual variability

Despite models being broadly able to capture ambient interannual variability (IAV) in aNPP ($r > 0.86$), they were seemingly unable to simulate observed treatment effects on IAV (noting the large observed treatment uncertainties). Directly assessing the models' ability to simulate observed treatment changes in IAV is not straightforward because it is not clear how the timing of growth relates to the timing of photosynthetic uptake. At the extreme, a number of models assume that one year's growth is entirely a product of the previous year's carbon uptake and thus meteorology. Other models modulate the growth–productivity relationships through the use of a labile C store. As a result, attempting to directly compare modelled time courses to growth observations is unproductive. To make progress we need more experimental insight into the time lag between productivity and growth. In this experiment, as is common, biomass and N concentration measurement were taken at the annual peak (mid-July). These measurements do not offer a constraint as we cannot separate direct responses from lagged effects.

C₃ vs. C₄ competition

During the course of the experiment, there were notable shifts in species dynamics. C₄ species initially prospered at the start of the experiment (Morgan *et al.*,

2011) but did worse than C3 species in the later years (Zelikova *et al.*, 2015; Mueller *et al.*, 2016). This shift is an important result with implications for future predictions of species composition and ecosystem function. In this study, models which had the capacity to simulate competition and associated recruitment (JULES, LPJ-GUESS, and SDGVM) did not, so they could be compared to other models without this functionality. Therefore, there remains an opportunity to further exploit the PHACE experimental data to test models that simulate C₃ vs. C₄ competition and to determine whether the experimental results are predictable. However, for such a comparison to be meaningful, the key identified issues with existing models when applied to this site will need to be tackled first.

Modelling in advance of experiments

In advance of the PHACE experiment, Parton *et al.* (2007) carried out a novel study in which they used DAYCENT to predict grassland responses to treatments. Studies like this can help identify testable predictions against which experimental data can then be compared (Norby *et al.*, 2016). Nevertheless, the Parton *et al.* (2007) study only used a single model, whereas a multimodel comparison (cf. Medlyn *et al.* 2016) would have identified a greater range of processes in which models differed, as this study demonstrates. *A priori* identification of areas where models diverge could have better helped guide experimentalists as to what key measurements would have helped constrain these model uncertainties. We strongly advocate the use of multimodel comparisons in advance of ecosystem-scale experiments (Medlyn *et al.*, 2016; Norby *et al.*, 2016); these studies need to become normal practice, rather than the exception.

Evaluation of models against multifactor experiments

Comparison of the models against the PHACE data has thus resulted in a clear agenda for improving model predictions of grassland response to environmental change. Interestingly, however, the multifactor nature of the experiment did not add greatly to the model evaluation. Global change will not affect a single factor in isolation, and thus, it is widely advocated that multifactor experiments be used to probe future changes in the terrestrial biosphere (Heimann & Reichstein, 2008; Luo *et al.*, 2008; Leuzinger *et al.*, 2011; Dieleman *et al.*, 2012). In our study, however, the multifactor comparison yielded little additional constraint on model responses, for several reasons.

One of the main reasons that multifactor experiments are commonly advocated is the need to

examine whether the main effects are additive or not when combined (Dieleman *et al.*, 2012; Mueller *et al.*, 2016). However, models rarely predict additive effects; rather, they predict nonlinear interactions, which can sometimes be too small to be detectable. In this study, models did not predict consistent interactions in response to combined treatments. Most models, in line with the observations, predicted greater than additive interactions in some years for both above- and below-ground biomass responses. Thus, determining whether or not main effects are additive is of little help to constrain models.

Interactive effects in multifactor experiments, particularly those carried out in environments that experience marked interannual variability in precipitation, are complex to interpret and it can be very challenging to identify the mechanisms underlying causing the observed responses. This statement is also true of the PHACE experiment, where treatment responses are overlaid on a marked year-to-year variability in responses to meteorology. Without a good causal understanding of the underlying processes, it is difficult to draw mechanistic understanding from the experiment that can be used to inform models.

However, the principal reason that the interacting responses did not help to constrain the models was because the models were unable to replicate the observed ecosystem behaviour under ambient conditions, or in response to single-factor treatments. As the interactive responses are contingent on key environmental factors such as soil water content and species composition, the models have to be able to realistically simulate these factors for their interactive effects to be comparable against data. Thus, at this stage, the most important way forwards is to use experimental data to improve model simulations of ambient conditions and responses to main effects (Norby & Luo, 2004). Future, improved, models, which are better able to simulate grassland phenology and can represent C₃ and C₄ competition, will likely find that the PHACE multifactor data set can provide a further constraint on our ability to predict response to global change.

Acknowledgements

Contributions from MDK, APW, XJY, KL, and RJN were supported by the U.S. Department of Energy Office of Science Biological and Environmental Research Programme. SZ was supported by the European Research Council (ERC) under the European Union's Horizon 2020 Research and Innovation Programme (QUINCY; grant no. 647204). XJL's contribution is supported by the CSIRO Postdoctoral Fellowship. We thank numerous individuals who made the PHACE experiment possible, especially Dana Blumenthal, Dan LeCain, Eric Hardy, and

David Smith. We also thank Kevin Mueller for sharing biomass data. AKJ was supported by the NSF (NSF AGS 12-43071), the US DOE (DOE DE-SC0016323) and NASA LCLUC program (NASA NNX14AD94G).

References

- Ahlström A, Raupach MR, Schurgers G *et al.* (2015) The dominant role of semi-arid ecosystems in the trend and variability of the land CO₂ sink. *Science*, **348**, 895–899.
- Botta A, Viovy N, Ciais P, Friedlingstein P, Monfray P (2000) Aglobal prognostic scheme of leaf onset using satellite data. *Global Change Biology*, **6**, 704–725.
- Carrillo Y, Dijkstra FA, Pendall E, Morgan JA, Blumenthal DM (2012) Controls over soil nitrogen pools in a semiarid grassland under elevated CO₂ and warming. *Ecosystems*, **15**, 761–774.
- Carrillo Y, Dijkstra FA, LeCain D, Morgan JA, Blumenthal D, Waldron S, Pendall E (2014) Disentangling root responses to climate change in a semiarid grassland. *Oecologia*, **175**, 699–711.
- Ciais P, Sabine C, Bala G *et al.* (2013) Carbon and other biogeochemical cycles. In: *Climate Change 2013: The Physical Science Basis. Contribution of Working Group I to the Fifth Assessment Report of the Intergovernmental Panel on Climate Change* (eds Stocker TF, Qin D, Plattner G-K, Tignor M, Allen SK, Boschung J, Nauels A, Xia Y, Bex V, Midgley PM), Cambridge University Press, Cambridge.
- Clark DB, Mercado LM, Sitch S *et al.* (2011) The joint UK land environment simulator (JULES), model description – part 2: carbon fluxes and vegetation dynamics. *Geoscientific Model Development*, **4**, 701–722.
- Cleveland CC, Townsend AR, Schimel DS *et al.* (1999) Global patterns of terrestrial biological nitrogen (N₂) fixation in natural ecosystems. *Global Biogeochemical Cycles*, **13**, 623–645.
- Cox PM (2001) *Description of the TRIFFID Dynamic Global Vegetation Model*. Hadley Centre Technical Note 24, Hadley Centre, Met Office, Bracknell, UK.
- De Kauwe MG, Medlyn BE, Zaehle S *et al.* (2013) Forest water use and water use efficiency at elevated CO₂: a model-data intercomparison at two contrasting temperate forest FACE sites. *Global Change Biology*, **19**, 1759–1779.
- De Kauwe MG, Medlyn BE, Zaehle S *et al.* (2014) Where does the carbon go? A model-data intercomparison of vegetation carbon allocation and turnover processes at two temperate forest free-air CO₂ enrichment sites. *New Phytologist*, **203**, 883–900.
- De Kauwe M, Zhou S-X, Medlyn B, Pitman A, Wang Y-P, Duursma R, Prentice I (2015) Do land surface models need to include differential plant species responses to drought? Examining model predictions across a mesic-xeric gradient in Europe. *Biogeosciences*, **12**, 7503–7518.
- Dentener F, Drevet J, Lamarque J *et al.* (2006) Nitrogen and sulfur deposition on regional and global scales: a multimodel evaluation. *Global Biogeochemical Cycles*, **20**, GB4003. doi: 10.1029/2005GB002672.
- Desborough C, Pitman A, Iranneiad P (1996) Analysis of the relationship between bare soil evaporation and soil moisture simulated by 13 land surface schemes for a simple non-vegetated site. *Global and Planetary Change*, **13**, 47–56.
- Dieleman WI, Vicca S, Dijkstra FA *et al.* (2012) Simple additive effects are rare: a quantitative review of plant biomass and soil process responses to combined manipulations of CO₂ and temperature. *Global Change Biology*, **18**, 2681–2693.
- Dijkstra FA, Blumenthal D, Morgan JA, Pendall E, Carrillo Y, Follett RF (2010) Contrasting effects of elevated CO₂ and warming on nitrogen cycling in a semiarid grassland. *New Phytologist*, **187**, 426–437.
- Dijkstra FA, Pendall E, Morgan JA *et al.* (2012) Climate change alters stoichiometry of phosphorus and nitrogen in a semiarid grassland. *New Phytologist*, **196**, 807–815.
- Dukes JS, Chiariello NR, Cleland EE *et al.* (2005) Responses of grassland production to single and multiple global environmental changes. *PLoS Biology*, **3**, e319.
- El Masri B, Shu S, Jai AK (2015) Implementation of a dynamic rooting depth and phenology into a land surface model: Evaluation of carbon, water, and energy fluxes in the high latitude ecosystems. *Agricultural and Forest Meteorology*, **211–212**, 85–99.
- Foley JA, Prentice IC, Ramankutty N *et al.* (1996) An integrated biosphere model of land surface processes, terrestrial carbon balance, and vegetation dynamics. *Global Biogeochemical Cycles*, **10**, 603–628.
- Franks P, Adams M, Amthor J *et al.* (2013) Sensitivity of plants to changing atmospheric CO₂ concentration: from the geological past to the next century. *New Phytologist*, **197**, 1077–1094.
- Friedlingstein P, Joel G, Field CB, Fung I (1998) Toward an allocation scheme for global terrestrial carbon models. *Global Change Biology*, **5**, 755–770.
- Fuhrer J (2003) Agroecosystem responses to combinations of elevated CO₂, ozone, and global climate change. *Agriculture, Ecosystems & Environment*, **97**, 1–20.
- Hadley M (1993) Grasslands for sustainable ecosystems. In: *Grasslands for Our World* (ed. Baker MJ), pp. 12–18. SIR Publishing, Wellington, NZ.
- Heimann M, Reichstein M (2008) Terrestrial ecosystem carbon dynamics and climate feedbacks. *Nature*, **451**, 289–292.
- Hovenden MJ, Newton P, Carran R *et al.* (2008) Warming prevents the elevated CO₂-induced reduction in available soil nitrogen in a temperate, perennial grassland. *Global Change Biology*, **14**, 1018–1024.
- Hovenden MJ, Newton PC, Wills KE (2014) Seasonal not annual rainfall determines grassland biomass response to carbon dioxide. *Nature*, **511**, 583–586.
- Hufkens K, Keenan TF, Flanagan LB *et al.* (2016) Productivity of North American grasslands is increased under future climate scenarios despite rising aridity. *Nature Climate Change*, **6**, 710–714.
- Jobbágy EG, Jackson RB (2000) The vertical distribution of soil organic carbon and its relation to climate and vegetation. *Ecological Applications*, **10**, 423–436.
- Kimball B (2005) Theory and performance of an infrared heater for ecosystem warming. *Global Change Biology*, **11**, 2041–2056.
- Knapp AK, Smith MD (2001) Variation among biomes in temporal dynamics of aboveground primary production. *Science*, **291**, 481–484.
- Knorr W, Kaminski T, Scholze M, Gobron N, Pinty B, Giering R, Mathieu P-P (2010) Carbon cycle data assimilation with a generic phenology model. *Journal of Geophysical Research: Biogeosciences*, **115**, G04017. doi: 10.1029/2009JG001119.
- Krinner G, Viovy N, de Noblet-Ducoudré N *et al.* (2005) A dynamic global vegetation model for studies of the coupled atmosphere-biosphere system. *Global Biogeochemical Cycles*, **19**, GB1015.
- Leuzinger S, Luo Y, Beier C, Dieleman W, Vicca S, Körner C (2011) Do global change experiments overestimate impacts on terrestrial ecosystems? *Trends in Ecology and Evolution*, **26**, 236–241.
- Lieth HFH (1978) *Patterns of Primary Productivity in the Biosphere*. Hutchinson Ross, Stroudsburg, PA.
- Luo Y, Gerten D, Le Maire G *et al.* (2008) Modelled interactive effects of precipitation, temperature, and [CO₂] on ecosystem carbon and water dynamics in different climatic zones. *Global Change Biology*, **14**, 1986–1999.
- Medlyn BE, Zaehle S, De Kauwe MG *et al.* (2015) Using ecosystem experiments to improve vegetation models. *Nature Climate Change*, **5**, 528–534.
- Medlyn BE, De Kauwe MG, Zaehle S *et al.* (2016) Using models to guide field experiments: *a priori* predictions for the CO₂ response of a nutrient- and water-limited native eucalypt woodland. *Global Change Biology*, **22**, 2834–2851.
- Melillo J, McGuire A, Kicklighter D, Moore B, Vorosmarty C, Schloss A (1993) Global climate change and terrestrial net primary production. *Nature*, **363**, 234–240.
- Migliavacca M, Galvagno M, Cremonese E *et al.* (2011) Using digital repeat photography and eddy covariance data to model grassland phenology and photosynthetic CO₂ uptake. *Agricultural and Forest Meteorology*, **151**, 1325–1337.
- Miglietta F, Hoosbeek M, Foot J *et al.* (2001) Spatial and temporal performance of the minifac (free air CO₂ enrichment) system on bog ecosystems in northern and central Europe. *Environmental Monitoring and Assessment*, **66**, 107–127.
- Milchunas D, Morgan J, Mosier A, LeCain D (2005) Root dynamics and demography in shortgrass steppe under elevated CO₂, and comments on minirhizotron methodology. *Global Change Biology*, **11**, 1837–1855.
- Morgan J, LeCain D, Pendall E *et al.* (2011) C4 grasses prosper as carbon dioxide eliminates desiccation in warmed semi-arid grasslands. *Nature*, **476**, 202–205.
- Mueller K, Blumenthal D, Pendall E *et al.* (2016) Impacts of warming and elevated CO₂ on a semi-arid grassland are non-additive, shift with precipitation, and reverse over time. *Ecology Letters*, **19**, 956–966.
- Norby RJ, Luo Y (2004) Evaluating ecosystem responses to rising atmospheric CO₂ and global warming in a multi-factor world. *New Phytologist*, **162**, 281–293.
- Norby RJ, De Kauwe MG, Domingues TF *et al.* (2016) Model-data synthesis for the next generation of forest free-air CO₂ enrichment (FACE) experiments. *New Phytologist*, **209**, 17–28.
- Oleson KW, Lawrence DM, Bonan GB *et al.* (2013) *Technical description of version 4.5 of the community land model (CLM)*. National Center for Atmospheric Research. Climate; Global Dynamics Division; Citeseer, National Center for Atmospheric Research, P.O. Box 3000, Boulder, Colorado.
- Parton WJ, Schimel DS, Cole C, Ojima D (1987) Analysis of factors controlling soil organic matter levels in great plains grasslands. *Soil Science Society of America Journal*, **51**, 1173–1179.
- Parton WJ, Scurlock JMO, Ojima DS *et al.* (1993) Observations and modeling of biomass and soil organic matter dynamics for the grassland biome worldwide. *Global Biogeochemical Cycles*, **7**, 785–809.
- Parton WJ, Morgan JA, Wang G, Del Grosso S (2007) Projected ecosystem impact of the prairie heating and CO₂ enrichment experiment. *New Phytologist*, **174**, 823–834.

- Pendall E, Heisler-White JL, Williams DG, Dijkstra FA, Carrillo Y, Morgan JA, LeCain DR (2013) Warming reduces carbon losses from grassland exposed to elevated atmospheric carbon dioxide. *PLoS ONE*, **8**, e71921.
- Pepper D, Del Grosso S, McMurtrie R, Parton W (2005) Simulated carbon sink response of shortgrass steppe, tallgrass prairie and forest ecosystems to rising [CO₂], temperature and nitrogen input. *Global Biogeochemical Cycles*, **19**, GB1004.
- Reyes-Fox M, Steltzer H, Trlica M, McMaster GS, Andales AA, LeCain DR, Morgan JA (2014) Elevated CO₂ further lengthens growing season under warming conditions. *Nature*, **510**, 259–262.
- Richardson AD, Hollinger DY, Dail DB, Lee JT, Munger JW, O'keefe J (2009) Influence of spring phenology on seasonal and annual carbon balance in two contrasting New England forests. *Tree Physiology*, **29**, 321–331.
- Riedo M, Gyalistras D, Grub A, Rosset M, Fuhrer J (1997) Modelling grassland responses to climate change and elevated CO₂. *Acta Oecologica*, **18**, 305–311.
- Ryan EM, Ogle K, Zelikova TJ, LeCain DR, Williams DG, Morgan JA, Pendall E (2015) Antecedent moisture and temperature conditions modulate the response of ecosystem respiration to elevated CO₂ and warming. *Global Change Biology*, **21**, 2588–2602.
- Scurlock J, Hall D (1998) The global carbon sink: a grassland perspective. *Global Change Biology*, **4**, 229–233.
- Shaw MR, Zavaleta ES, Chiariello NR, Cleland EE, Mooney HA, Field CB (2002) Grassland responses to global environmental changes suppressed by elevated CO₂. *Science*, **298**, 1987–1990.
- Smith B, Wärlind D, Arneth A, Hickler T, Leadley P, Silberg J, Zaehle S (2014) Implications of incorporating N cycling and N limitations on primary production in an individual based dynamic vegetation model. *Biogeosciences*, **11**, 2027–2054.
- Song Y, Jain AK, McIsaac GF (2013) Implementation of dynamic crop growth processes into a land surface model: evaluation of energy, water and carbon fluxes under corn and soybean rotation. *Biogeosciences*, **10**, 8039–8066.
- Verhoef A, Egea G (2014) Modeling plant transpiration under limited soil water: comparison of different plant and soil hydraulic parameterizations and preliminary implications for their use in land surface models. *Agricultural and Forest Meteorology*, **191**, 22–32.
- Walker AP, Beckerman AP, Gu L *et al.* (2014) The relationship of leaf photosynthetic traits – V_{cmax} and J_{max} – to leaf nitrogen, leaf phosphorus, and specific leaf area: a meta-analysis and modeling study. *Ecology and Evolution*, **4**, 3218–3235.
- Walker AP, Zaehle S, Medlyn BE *et al.* (2015) Predicting long-term carbon sequestration in response to CO₂ enrichment: how and why do current ecosystem models differ? *Global Biogeochemical Cycles*, **29**, 476–495.
- Wang Y-P, Trudinger CM, Enting IG (2009) A review of applications of model-data fusion to studies of terrestrial carbon fluxes at different scales. *Agricultural and Forest Meteorology*, **149**, 1829–1842.
- White MA, Thornton PE, Running SW *et al.* (2000) Parameterization and sensitivity analysis of the BIOME-BGC terrestrial ecosystem model: net primary production controls. *EarthInteractions*, **4**, 1–85.
- Woodward FI, Lomas MR (2004) Vegetation dynamics – simulating responses to climatic change. *Biological Reviews*, **79**, 643–670.
- Zaehle S, Friend AD (2010) Carbon and nitrogen cycle dynamics in the O-CN land surface model: 1. Model description, site-scale evaluation, and sensitivity to parameter estimates. *Global Biogeochemical Cycles*, **24**, GB1005, doi: 10.1029/2009GB003521.
- Zaehle S, Medlyn BE, De Kauwe MG *et al.* (2014) Evaluation of 11 terrestrial carbon–nitrogen cycle models against observations from two temperate free-air CO₂ enrichment studies. *New Phytologist*, **202**, 803–822.
- Zhang H (2004) Analyzing the potential impacts of soil moisture on the observed and model-simulated Australian surface temperature variations. *Journal of Climate*, **17**, 4190–4212.
- Zelikova TJ, Williams DG, Hoenigman R, Blumenthal DM, Morgan JA, Pendall E (2015) Seasonality of soil moisture mediates responses of ecosystem phenology to elevated CO₂ and warming in a semi-arid grassland. *Journal of Ecology*, **103**, 1119–1130.
- Zhou S, Duursma RA, Medlyn BE, Kelly JW, Prentice IC (2013) How should we model plant responses to drought? An analysis of stomatal and non-stomatal responses to water stress. *Agricultural and Forest Meteorology*, **182–183**, 204–214.
- Zhou S, Medlyn B, Sabaté S, Sperlach D, Prentice IC (2014) Short-term water stress impacts on stomatal, mesophyll and biochemical limitations to photosynthesis differ consistently among tree species from contrasting climates. *Tree Physiology*, **10**, 1035–1046.

Supporting Information

Additional Supporting Information may be found in the online version of this article:

Figure S1. Ratio of above- and below-ground biomass in the control (ct) treatment.

Figure S2. Reduction in gas exchange (β) with declining soil moisture content in 2007 and 2009.

Figure S3. Response of nitrogen use efficiency to CO₂ (Ct), warming (cT) and CO₂ × warming (CT).

Figure S4. Response of nitrogen uptake to CO₂ (Ct), warming (cT) and CO₂ × warming (CT).

Figure S5. Response of nitrogen mineralization to CO₂ (Ct), warming (cT) and CO₂ × warming (CT).

Table S1. Number of days change in leaf onset in the CO₂ (Ct), warming (cT) and CO₂ × warming treatments. Positive numbers indicate earlier onset dates. CABLE and SDGVM have been excluded, as they do not completely drop their leaves. CLM4.5 has also been excluded as the C₃ grasses did not grow and it is clear that the C₄ grass phenology does not work at this site (Fig. 3).

Table S2. Number of days change in leaf senescence in the CO₂ (Ct), warming (cT) and CO₂ × warming treatments. CABLE and SDGVM have been excluded, as they do not completely drop their leaves. CLM4.5 has also been excluded as the C₃ grasses did not grow and it is clear that the C₄ grass phenology does not work at this site (Fig. 3).